Journal of Hydrology 593 (2021) 125766

Contents lists available at ScienceDirect

Journal of Hydrology

journal homepage: www.elsevier.com/locate/jhydrol

Research papers

Tracing source and transformation of carbon in an epikarst spring-pond system by dual carbon isotopes (^{13}C—^{14}C): Evidence of dissolved CO_2 uptake as a carbon sink

Bo Chen [a,b], Min Zhao [a,*], Hao Yan [a], Rui Yang [b], Hong-Chun Li [c,d,**], Douglas E. Hammond [e]

[a] State Key Laboratory of Environmental Geochemistry, Institute of Geochemistry, CAS, Guiyang 550081, China
[b] College of Public Management, Guizhou University of Finance and Economics, Guiyang 550025, Guizhou, China
[c] Department of Geosciences, National Taiwan University, Taipei 10617, Taiwan
[d] Frontiers Science Center for Deep Ocean Multispheres and Earth System, Key Laboratory of Marine Chemistry Theory and Technology, Ministry of Education, Ocean University of China, Qingdao 266100, China
[e] Department of Earth Sciences, University of Southern California, Los Angeles, CA 90089-0740, USA

ARTICLE INFO

This manuscript was handled by Corrado Corradini, Editor-in-Chief, with the assistance of Jongjun Jiang, Associate Editor

Keywords:
Karst surface water
DIC
POC
Stable carbon isotope
Radiocarbon
Aquatic photosynthesis

ABSTRACT

$\delta^{13}C$ and $D^{14}C$ measurements on dissolved inorganic carbon (DIC), particulate organic carbon (POC) and aquatic plants from a karst spring and two spring-fed ponds in Laqiao, Maolan Township, Libo County, southeastern Guizhou of China in January, July and October of 2013 have been carried out to understand the roles of aquatic photosynthesis through DIC uptake in surface karst waters. The mean $D^{14}C$ and $\delta^{13}C$ values of DIC for the spring, midstream pond (MP) and downstream pond (DP) are -26 ± 36‰ and -13 ± 2‰, 6 ± 56‰ and -12 ± 3‰, and 0 ± 64‰ and -9 ± 2‰, respectively. The carbon source for the DIC is mainly from biogenic CO_2 rather than the dissolution of limestone rock as the $D^{14}C$ and $\delta^{13}C$ of limestone are about -1000‰ and 2‰, respectively. The enrichment trend of $D^{14}C_{DIC}$ and $\delta^{13}C_{DIC}$ from the spring to the DP indicates CO_2 exchange between atmospheric CO_2 and DIC, because $D^{14}C$ and $\delta^{13}C$ values of atmospheric CO_2 are ca. 50‰ and -8‰, respectively. The average $D^{14}C_{POC}$ values in the spring, MP and DP were -325‰, -123‰ and -158‰, respectively, which are all lower than these of the DIC in each reservoir. The lower $D^{14}C$ values of the POC may be caused by older soil carbon from surface runoff and dust fall. More aquatic algae were formed through photosynthesis in the stream ponds, especially in summer, shown by strongly increased $D^{14}C_{POC}$ and evidence of growth in EDS/SEM analyses. Furthermore, the $D^{14}C$ values of the submerged aquatic plants range from -153‰ to -26‰, reflecting that the aquatic plants used DIC for photosynthesis. The $D^{14}C$ value of an emergent plant which uses atmospheric CO_2 during photosynthesis is 52.5 ± 0.3‰, equivalent to the atmospheric $D^{14}C$. Seasonal variations of $D^{14}C_{DIC}$ and $\delta^{13}C_{DIC}$ are influenced by soil CO_2 input, primary productivity in the ponds, and CO_2 exchange; hydrochemical condition show lower $D^{14}C$ values but higher $\delta^{13}C$ values in cold/dry season, and vice versa in summer rainy season. A simple mass balance calculation indicates ~90% of carbon for the spring DIC is from biogenic CO_2, with higher contribution in summer due to higher productivity. Although this simple calculation may overestimate the biogenic CO_2, it indicates that organic decomposition is a major carbon source for DIC in the karst hydrological system. The results of the present study have implications for ^{14}C dating on aquatic plant remains, regional and perhaps global carbon budgets, and the different behaviors of ^{13}C and ^{14}C in karst systems.

1. Introduction

Sourced from watershed inputs and influenced by fluvial processes (Sun et al., 2015), riverine input of dissolved and particulate carbons to oceans can play an important role in regional and global carbon budgets (Meybeck, 1982; Degens et al., 1991; Marwick et al., 2015; Xue et al., 2017; Ge et al., 2020). For most rivers, dissolved inorganic carbon (DIC) that is dominated by bicarbonate ion comes mainly from chemical weathering of carbonates and silicates in their drainage basins. There are complex processes involved in the DIC cycling in river systems,

* Corresponding author.
** Correspondence to: H-C Li, Department of Geosciences, National Taiwan University, Taipei 10617, Taiwan.
E-mail addresses: zhaomin@vip.gyig.ac.cn (M. Zhao), hcli1960@ntu.edu.tw (H.-C. Li).

https://doi.org/10.1016/j.jhydrol.2020.125766
Received 29 September 2020; Received in revised form 9 November 2020; Accepted 10 November 2020
Available online 18 November 2020

including oxidation of organic matter, precipitation or dissolution of carbonates, CO_2 exchange with the atmosphere and photosynthesis (Buhl et al., 1991; Aucour et al., 1999; Sun et al., 2011; Liu et al., 2017).

Falkowski and Raven (2007) estimated that approximately 50% of the photosynthesis on Earth occurs in aquatic environments. Therefore, aquatic carbon fixation is particularly relevant in the regulation of the global carbon cycles. The role of ocean aquatic photosynthesis in the uptake of CO_2 and/or HCO_3^- has been studied intensively (e.g., Falkowski, 1997; Cassar et al., 2004; Tortell et al., 2008). On the other hand, the role of terrestrial aquatic photosynthesis in the CO_2 uptake is more complicated and less studied. How does terrestrial aquatic photosynthesis utilize DIC to form the autochthonous organic carbon? And, what is the carbon budget of terrestrial aquatic systems in global carbon cycles? Because karst water system contains abundant DIC in natural waters, carbon sources and their transformation as well as aquatic photosynthesis are particularly important in regional carbon budgets (Liu et al., 2010, 2015; Liu, 2013; Liu and Dreybrodt, 2015). In studies of the Xijiang River and its tributaries in a karst area of SW China, Sun et al. (2011, 2015) pointed out that the fractions transformed from carbonate-sourced DIC through photosynthesis of aquatic organisms ranged from 3.4% to 20.5% in the rainy season, and from 12.3% to 22.1% in the dry season, implying an important sink of atmospheric CO_2 in river systems. However, the process of transformation from DIC into organic carbon in karst water is still poorly understood.

Carbon isotopes are often used for tracing carbon sources and isotopic fractionations among phases and/or materials in natural water systems (e.g., Taylor and Fox, 1996; Yang et al., 1996; Atekwana and Krishnamurthy, 1998; Amiotte-Suchet et al., 1999; Aucour et al., 1999; Das et al., 2005; Han et al., 2010; Kanduč et al., 2012; Tsypin and Macpherson, 2012; Zhao et al., 2015a). However, using only $\delta^{13}C$ in tracing carbon sources often encounters problems associated with source and process overlaps (Raymond and Bauer, 2001a). Radiocarbon isotope (^{14}C) has a much greater dynamic range (−1000‰ to 200‰) compared to $\delta^{13}C$ (−40‰ to 2‰), and offers a particularly powerful tracer of the origin of C pools and their cycling within aquatic ecosystems (Raymond et al., 2004; Sun et al., 2015; Marwick et al., 2015; Ishikawa et al., 2015; Liu et al., 2017). Thus, combining $\delta^{13}C$ and $D^{14}C$ values in different carbon species (DIC, POC, dissolved organic carbon (DOC), and plants) can certainly provide much more detailed information on the source, age, residence time and transformation of carbon in an aquatic system and can overcome problems associated with source overlap (Raymond and Bauer, 2001a, 2001b, 2001c).

The present study uses stable and radioactive carbon isotopes (^{13}C—^{14}C) of DIC, POC and aquatic plants in a karst aquatic system in southwestern China for identifying carbon sources and processes of carbon transformation. This study aims to identify the contribution of aquatic photosynthesis in the carbon cycle of this setting.

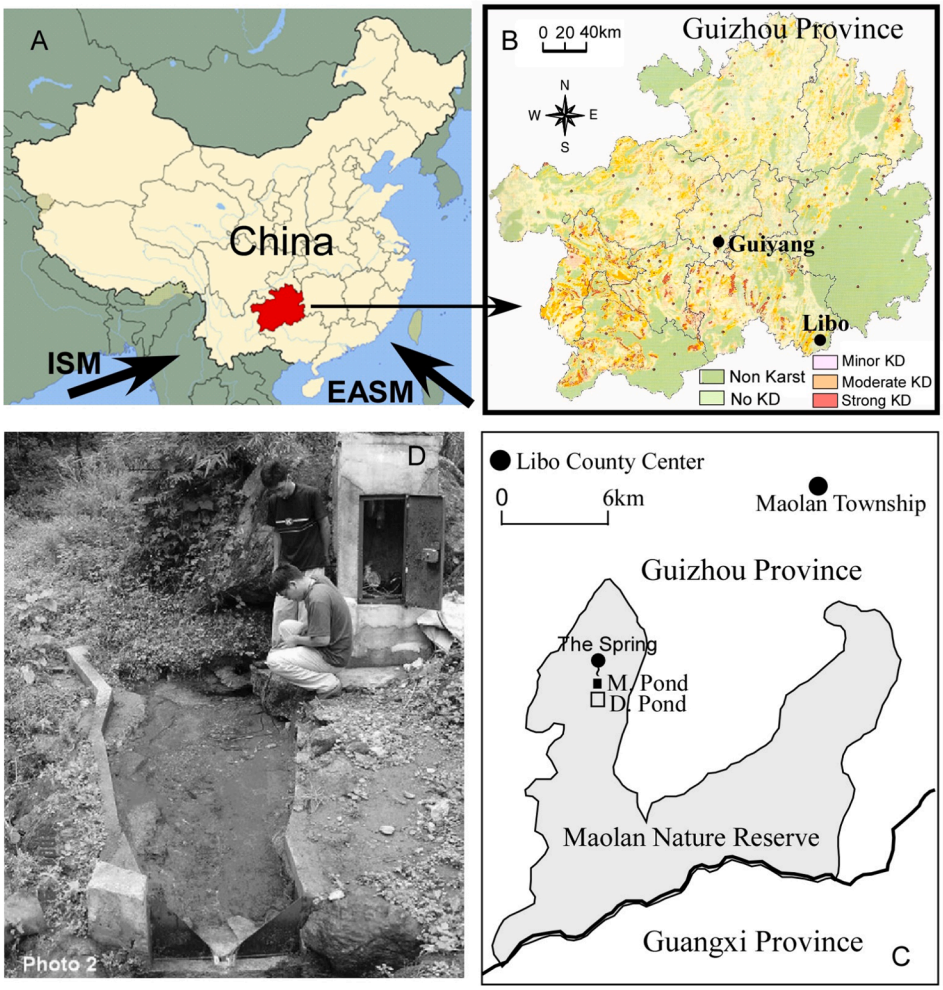

Fig. 1. Geographic location of the study site (modified from Jiang et al., 2008; Chen et al., 2014). (A) Location of Guizhou in China. ISM and EAMS denote Indian Summer Monsoon and East Asian Summer Monsoon, respectively. (B) Location of Libo County in Guizhou. Color codes in the map indicate the degrees of karst-desertification (KD) (Kuo et al., 2011 and references therein). (C) Map of the study area. (D) Picture of the spring monitoring site (copied from Liu et al., 2007).

2. Study site

Located in Libo county of Guizhou Province in SW China, Maolan National Reserve is well known for its dense virgin evergreen forests growing on cone karst and is listed by the United Nations Educational, Scientific and Cultural organization (UNESCO) as a world nature heritage site (Libo Karst, one of the three clusters of South China Karst, whc.unesco.org) (Fig. 1). With a subtropical monsoon climate, the average annual rainfall in the virgin forest area is about 1750 mm, nearly 80% of precipitation occurring in the monsoon season from April to September, and the annual mean air temperature is about 17 °C (Zhou, 1987). The lithology in this area is mainly dolomitic limestone of Middle and Lower Carboniferous age (Jiang et al., 2008; Liu et al., 2007; Han et al., 2010; Chen et al., 2014). Soils in the study area are relatively thin and discontinuous with thickness of 30–40 cm, often existing in rock fractures. However, a unique natural complexity of karst forest appears in this karst geomorphological setting under subtropical monsoons (Zhou, 1987). The forest contains mixed deciduous broadleaved trees which form a stable ecosystem.

Maolan Spring, is a Ca-HCO_3 type epikarst spring with flow rates that vary from 0.05 to 3 L/s during the year (Liu et al., 2007). It is situated at the base of a cone karst slope that is covered by virgin karst forest. Fig. 2 shows full views of the spring channel and the receiving ponds (MP = midstream pond and DP = downstream pond). A large quantity of submerged plants (chiefly *Hydrilla verticillata*) grows in MP. In the spring, some submerged plants (chiefly *Charophyta*) exist, whereas no submerged plants appear in DP. Weirs were built to control spring and pond outflows. The weir for the spring was built in 2002 for long-term monitoring of water stage and flow calculation (Liu et al., 2007), whereas the weirs for MP and DP were built in 2004 but have only been monitored since 2011 (Liu et al., 2015).

Water from the spring at the monitoring site (Fig. 1D) flows into a channel and enters a small pool (Fig. 2 Spring channel), then enters the MP. The distance from the spring outlet and MP is 38 m. The water chemistry and flow rate of the spring were monitored at the spring outlet (Fig. 1D). All water, POC and plant samples for the spring were also collected at the site shown in Fig. 1D. The volume of the spring reservoir is rather small with 0.5 × 2 m in area and <0.5 m deep, which approximately yields a volume <0.5 m^3. The average spring discharge

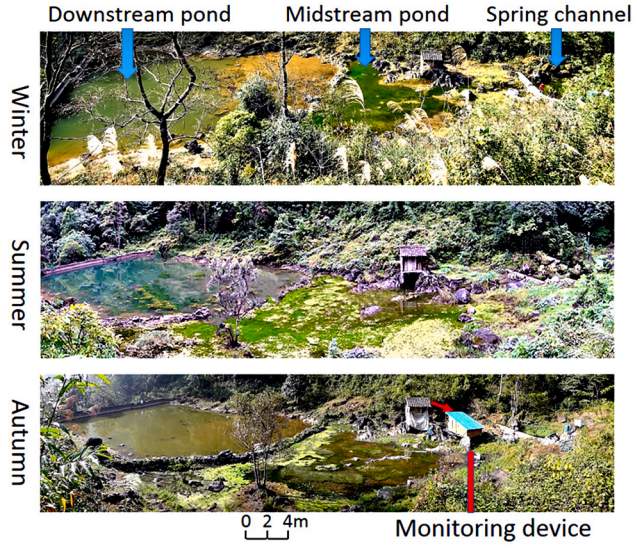

Fig. 2. Full views of Maolan Spring and the spring-fed two ponds in winter, summer and autumn months. Aquatic plants are very abundant in the midstream pond. The cabin with 2 m wide, 2 m long and 3 m tall in each photo was built for monitoring device in 2004. Then, the monitoring device for MP and DP was transferred into a new cabin in 2011 shown in the lower panel.

was 0.6 L/s in January, 2 L/s in July and 0.9 L/s in October, with relatively stable flow rates during each month. The areas of MP and DP were 280 m^2 and 1300 m^2 respectively. The water depth of MP is shallow, so that its volume is much smaller (about 60 m^3) than that of DP (nearly 1300 m^3) (Chen et al., 2014; Liu et al., 2015). The spring and pond setting is an ideal natural monitoring system for study of carbon cycle and transformation in surface karst water.

Water from the spring enters the MP and DP directly with very short residence time, the ponds have the same environment. No other underground flows enter the ponds. Although the influence of surface runoff and direct rainfall on the hydrological system was not quantified, there was no rainfall recorded during the sampling dates. In the rainy season, water chemistry of DP may be buffered by its large size compared to the MP. Using the fore-mentioned spring flow rates, we can estimate the water residence time in MP was 28 h in January, 8 h in July and 19 h in October, considering no evaporation and other inputs. For DP, the estimated residence time was 25 days in January, 7.5 days in July and 17 days in October. The above estimation indicates that water residence time in MP was much shorter than that in DP, so that the effects of environmental influence on water chemistry and biological activity between MP and DP are different.

3. Methods

3.1. Sample collection and pretreatment

Measurements of hydrochemical parameters (flow rate, temperature, pH, conductivity, dissolved oxygen, and ions) and collections of samples (DIC, POC, plants) from the spring and the two spring-fed ponds were conducted during 27–28 January (winter), 24–25 July (summer) and 24–25 October (autumn) of 2013. Water samples for $\delta^{13}C_{DIC}$ and $D^{14}C_{DIC}$ were collected in pre-cleaned evacuated 60 mL glass vials, with no air space. One drop of saturated $HgCl_2$ solution was added to each sample to prevent microbial activity, and samples were kept at 4 °C in the laboratory until analysis. The preserved samples for $\delta^{13}C_{DIC}$ and $D^{14}C_{DIC}$ analyses were acidified with pure phosphoric acid (Raymond et al., 2004), and then evolved CO_2 was purified on a vacuum extraction line after cryogenic removal of H_2O using a liquid nitrogen-ethanol trap.

Water samples were filtered by a vacuum filtration device through 0.7 μm Whatman GF/F filter papers (47 mm in diameter) which were pre-weighed after combustion at 450 °C for 6 h. The GF/F filter papers were freeze-dried and analyzed for POC after removing the inorganic carbon by reaction with HCl fumes in the State Key Laboratory of Environmental Geochemistry (EG Lab) at the Institute of Geochemistry, Chinese Academy of Science, Guiyang. The treated POC samples on the papers were then combusted with CuO powder and Ag wire at 850 °C in an evacuated 9 mm quartz tube in the Accelerator Mass Spectrometer (AMS) Radiocarbon Dating Laboratory of the National Taiwan University (NTUAMS Lab). Yields of CO_2 were quantified using an absolute pressure gauge on a vacuum extraction line, and aliquots were taken for $D^{14}C$ measurements by AMS at NTUAMS Lab and for $\delta^{13}C$ measurements by IRMS in the EG Lab.

Plant samples collected from the spring and MP were pretreated in the NTUAMS Lab following the standard ^{14}C methods of Oxford Radiocarbon Accelerator Unit (ORAU) to ensure that any adsorbed carbon dioxide was removed (Brock et al., 2010). Samples were rinsed with distilled water and freeze-dried prior to combustion and graphitization. The dried samples (~2 mg) were then treated using the same procedures used for POC samples.

3.2. In situ titration and chemical analysis

Field titrations were used to measure the alkalinity and [Ca^{2+}] of water, with the Aquamerck Alkalinity Test and Hardness Test. Since the majority of dissolved inorganic carbon species in the karst water when pH is around 8, the alkalinity measurement is close to [HCO_3^-]. In the

karst environment, Ca^{2+} and Mg^{2+} are the major ions, but [Ca^{2+}] is 2–3 times larger than [Mg^{2+}]. Thus, we use the results of the Alkalinity Test and Hardness Test as the results of [HCO_3^-] and [Ca^{2+}] measurements. The precisions for [HCO_3^-] and [Ca^{2+}] measurements are 6 mg/L and 1 mg/L, respectively. Two sets of 60-ml samples were transferred in acid-washed hydroplastic bottles for chemical analysis of cations and anions after filtering through 0.45 μm Millipore filters. The samples for cation analysis were acidified to pH <2.0 using concentrated nitric acid. Parameters of temperature, pH, electronic conductivity (EC) and dissolved oxygen (DO) were measured in situ by a hand-held WTW 350 water quality meter with 1σ error of <2%.

The water samples were taken back to the EG Lab to determine cation concentrations of Na^+, K^+, Ca^{2+} and Mg^{2+} through an inductively coupled plasma optical emission spectrometer (ICP-OES) and anion concentrations of SO_4^{2-}, Cl^-, and NO_3^- by a Dionex ICS-90 ion chromatography. All measured hydrochemical parameters are listed in Tables 1 and 2. Since the concentrations of K^+, Na^+, Ca^{2+}, Mg^{2+}, Cl^-, SO_4^{2-}, NO_3^- and HCO_3^- did not vary significantly for each reservoir during each sampling month, Table 2 lists only the average values of them. From Table 2, one can see Ca^{2+} is the major cation and HCO_3^- is the major anion, which is the feature of karst hydrology.

3.3. Calculating CO_2 partial pressure and calcite saturation index

CO_2 partial pressure (pCO_2) and the calcite saturation index (SI_C) are calculated from a geochemical model with pH, temperature and concentrations of seven major ions (Liu et al., 2007; Zhao et al., 2010, 2015a). Since the host rocks in the study region are limestone and dolomite, intercalated with gypsum strata, Ca^{2+}, Mg^{2+}, HCO_3^- and SO_4^{2-} are the major ions. With the recorded temperature and pH, as well as the measured ion concentrations, calculations of pCO_2 and SI_C were processed through the program WATSPEC (Wigley, 1977) based on the following equations:

$$pCO_2 = (HCO_3^-)(H^+)/(K_1 * K_{CO2}) \quad (1)$$

$$SI_C = log\left[(Ca^{2+})(CO_3^{2-})/K_C\right] \quad (2)$$

where K_1, K_{CO2} and K_C are the equilibrium constants for carbonic acid (H_2CO_3), CO_2 and calcite dissolution, respectively. If $SI_C > 0$, water is supersaturated with respect to calcite and if $SI_C < 0$, water is undersaturated. The calculated pCO_2 and SI_C values are listed in Table 1.

3.4. Continuous monitoring of daily variations in hydrochemical conditions

Diurnal cycles of the 3 water bodies were monitored in 3 seasons. In-situ hydrochemical parameters (temperature, pH, EC and DO) were measured every 15 min using a WTW 350i Multiline P3 automated device. Two to three water samples for $\delta^{13}C_{DIC}$ analyses were collected over the course of a day. Table 3 lists the hydrochemical parameters corresponding to the $\delta^{13}C_{DIC}$ samples. The monitoring device (WTW) for the DP was broken at 14:00 PM in the afternoon of 10/25/2013, so that there was no hydrochemical record for the last five $\delta^{13}C_{DIC}$ samples of the DP in Table 3.

3.5. Carbon isotopic analysis

POC and plant samples were combusted by the method described in Section 3.1, and the purified CO_2 was sealed in a glass tube for $\delta^{13}C$ measurement. The $\delta^{13}C_{DIC}$, $\delta^{13}C_{POC}$, and $\delta^{13}C_{plant}$ were determined on a MAT-252 mass spectrometer with dual inlet in the EG Lab. Results are in Tables 3 and 4, relative to V-PDB (‰), and have ~0.15‰ (1σ) precision.

The purified CO_2 of DIC, POC and plant samples for $D^{14}C$ measurements were placed on the graphitization line under vacuum of 10^{-3} mbar in the NTUAMS Lab. When exposed to 400 mg Zn at 450 °C for reaction, the CO_2 was reduced to graphite with Fe (Fe:C = 3.5:1) under 550 °C for 6–8 h. Graphite samples were pressed into targets and measured for their $^{14}C/^{12}C$ and $^{13}C/^{12}C$ ratios with a 1.0 MV Tandetron Model 4110 BO-AMS made by High Voltage Engineering Europa B.V. (HVEE) in the NTUAMS Lab. Each batch of sample targets was run with three targets of oxalic acid standards (OXII, 4900C), three targets of carbonate backgrounds (NTUB), and two targets of inter-comparison samples. All standard, background and inter-comparison targets were processed with the same procedures as the sample targets. All reported

Table 1
Hydrochemical parameters and $\delta^{13}C_{DIC}$ values of the water samples from the study sites in different seasons. Water temperature (T), pH, electrical conductivity (EC) and dissolved oxygen (DO) were measured by an automatic WTW device in situ. Ca^{2+} and alkalinity were measured by titration in the field. SI_C and pCO_2 were calculated by the WATSPEC program. $\delta^{13}C_{DIC}$ values of water samples were measured by a MAT 252 IRMS.

Date	Time	T (°C)	pH	EC (μs/cm)	DO (mg/L)	Ca^{2+} (mg/L)	Alkalinity (mg/L)	SI_C	pCO_2 (ppm)	$\delta^{13}C_{DIC}$ (‰)
Spring										
20130127	12:00	15.7	8.14	328	8.6	70	195	0.7	1191	−11.18
20130725	08:00	17.8	7.23	361	6.3	53	223	−0.2	11,668	−15.26
20130724	20:00	17.5	7.20	363	6.1	54	224	−0.3	12,274	−15.05
20131025	08:00	16.9	7.65	381	7.6	62	238	0.3	4645	−12.63
20131025	15:00	17.5	7.70	378	8.0	58	226	0.3	3954	−12.17
20131025	18:00	17.4	7.73	377	8.1	56	238	0.3	3890	−12.06
Midstream pond										
20130127	18:00	15.5	9.03	251	12.8	44	146	1.2	101	−6.75
20130128	08:00	10.9	7.87	271	9.0	48	153	0.1	1690	−8.68
20130724	14:00	30.8	8.98	316	15.1	46.6	194	1.4	171	−11.86
20130725	08:00	24.4	7.53	335	0.7	49.5	206	0.1	6012	−15.15
20130725	12:00	27.9	9.00	320	11.9	47.2	197	1.4	160	−13.90
20131025	08:00	14.4	8.01	320	2.4	46	177	0.3	1462	−12.84
20131025	12:00	17.1	9.18	234	3.0	34	171	1.3	80	−10.96
20131025	15:00	22.1	9.27	201	1.4	18	116	1	45	−9.92
20131025	18:00	21.8	9.83	180	12.6	16	110	1.2	7	−10.41
Downstream pond										
20130127	12:00	10.5	8.30	295	9.7	50	183	0.6	735	−7.92
20130127	18:00	12.8	8.35	289	10.2	46	177	0.6	647	−7.93
20130128	08:00	10.4	8.27	294	9.6	48	183	0.6	789	−7.99
20130724	14:00	30.0	8.37	289	8.6	42.6	177	0.9	755	−12.05
20130725	08:00	26.7	8.16	293	8.2	43.2	180	0.7	1280	−12.38
20131025	08:00	10.8	8.34	293	10.0	48	177	0.6	647	−8.93
20131025	15:00	21.5	8.41	337	5.7	48	207	0.9	718	−8.36

Table 2
Average concentrations of cations and anions measured by an inductively coupled plasma optical emission spectrometer (ICP-OES) and a Dionex ICS-90 ion chromatography. Concentrations of HCO_3^- are averaged from the alkalinity measurements in the field. All values are in mg/L.

Time	Pond	K^+	Na^+	Ca^{2+}	Mg^{2+}	Cl^-	SO_4^{2-}	NO_3^-	HCO_3^-
January	SP	0.23	0.40	49.41	15.77	1.01	5.64	12.19	202
	MP	0.33	0.42	34.13	15.98	1.06	2.21	11.86	163
	DP	0.21	0.36	40.71	16.59	0.92	2.22	13.23	180
July	SP	n.a.	n.a.	53.58	16.87	0.61	3.53	12.72	224
	MP	0.52	n.a.	44.72	17.77	1.86	0.24	8.57	186
	DP	n.a.	n.a.	43.69	17.09	0.89	1.13	9.86	182
October	SP	0.16	0.39	55.41	15.26	1.05	12.09	5.39	234
	MP	0.17	0.38	53.98	15.37	0.95	13.01	2.43	139
	DP	0.21	0.37	52.15	15.39	1.08	12.82	3.44	208

Table 3
Diurnal variations of the hydrochemical parameters and $\delta^{13}C_{DIC}$ in the spring pool, midstream pond, and downstream pond at the study site. Water temperature (°C), pH, electronic conductivity (μs/cm) and dissolved oxygen (mg/L) were measured every 15 min by an automatic WTW device in each reservoir respectively. The $\delta^{13}C_{DIC}$ (‰, V-PDB) of the water samples were measured by a MAT 252 IRMS.

Date	Time	T (°C)	pH	EC (us/cm)	DO (mg/L)	$\delta^{13}C_{DIC}$ (‰)	T (°C)	pH	EC (us/cm)	DO (mg/L)	$\delta^{13}C_{DIC}$ (‰)	T (°C)	pH	EC (us/cm)	DO (mg/L)	$\delta^{13}C_{DIC}$ (‰)
		Spring					Midstream pond					Downstream pond				
20130127	12:00	15.7	8.14	328	8.6	−11.11	11.9	8.34	287	10.0	−8.56	10.5	8.30	295	9.7	−7.92
20130127	14:00	15.9	8.13	328	8.5	−11.35	14.9	8.78	278	12.5	−6.18	11.4	8.30	295	9.9	−7.8
20130127	16:00	15.7	8.14	329	8.6	−11.10	16.6	9.06	263	13.3	−7.08	12.6	8.30	293	10.0	−7.59
20130127	18:00	15.6	8.19	329	8.9	−10.96	15.5	9.03	251	12.8	−6.75	12.8	8.35	289	10.2	−7.93
20130127	21:00	15.4	8.10	329	8.2	−11.16	14.1	8.99	243	13.5	−7.88	11.8	8.31	292	9.9	−7.98
20130128	00:00	15.3	8.05	330	8.0	−11.23	12.9	8.82	247	13.0	−8.30	11.3	8.31	292	9.7	−8.18
20130128	04:00	15.3	8.03	331	8.0	−11.26	11.8	8.43	254	10.7	−8.32	10.6	8.29	294	9.6	−8.14
20130128	09:00	15.3	8.08	330	8.5	−11.26	11.1	8.06	282	9.0	−8.68	10.3	8.28	294	9.6	−7.99
20130128	13:00	15.5	8.17	328	9.2	−11.21	11.5	8.50	292	9.7	−8.79	10.7	8.31	294	9.9	−8.05
20130724	14:00	17.6	7.22	362	6.4	−15.04	30.6	9.03	316	14.9	−11.86	30.0	8.37	289	8.6	−12.05
20130724	20:00	17.5	7.20	363	6.1	−15.05	28.0	8.91	280	15.0	−12.20	29.1	8.39	297	7.4	−12.07
20130725	08:00	17.8	7.23	361	6.3	−15.26	24.3	7.50	335	0.4	−15.15	26.7	8.16	293	8.2	−12.38
20130725	12:00	17.7	7.22	362	6.1	−15.07	28.3	8.98	324	15.7	−13.90	28.2	8.24	297	9.3	−12.23
20131024	15:00	17.6	7.69	379	8.1	−12.37	22.0	9.26	211	20.4	−11.70	20.2	8.40	333	6.5	−8.76
20131024	16:00	17.6	7.68	378	8.1	−12.40	22.2	9.21	192	19.5	−10.65	20.3	8.44	339	5.8	−8.76
20131024	17:00	17.6	7.69	379	8.1	−12.39	21.7	9.31	185	19.8	−10.70	19.9	8.46	339	5.7	−8.79
20131024	18:00	17.5	7.69	379	8.2	−12.89	21.1	9.43	183	19.0	−10.98	19.5	8.45	339	6.1	−8.91
20131024	20:00	17.4	7.69	379	7.7	−12.15	19.7	9.18	191	17.9	−11.14	18.7	8.34	340	5.7	−8.39
20131024	22:00	17.3	7.66	380	6.7	−12.28	18.4	9.09	200	17.7	−11.57	18.2	8.33	339	5.6	−8.63
20131025	00:00	17.2	7.62	380	6.8	−12.61	17.4	8.73	212	13.2	−11.89	17.7	8.33	338	5.8	−8.73
20131025	02:00	17.1	7.64	381	6.8	−13.34	16.4	8.32	233	11.8	−12.31	17.3	8.33	339	5.6	−8.80
20131025	07:00	17.0	7.70	381	6.8	−12.76	14.4	8.01	320	2.4	−13.24	16.5	8.17	340	4.9	−8.83
20131025	08:00	17.1	7.72	378	8.2	−12.63	14.1	8.04	325	2.1	−12.84	16.4	8.19	340	4.4	−8.93
20131025	09:00	17.5	7.68	378	7.9	−12.47	14.4	8.31	325	2.5	−12.67	16.7	8.23	340	4.9	−8.84
20131025	10:00	17.5	7.68	378	7.9	−12.20	15.0	7.91	245	1.9	−12.39	16.9	8.28	339	4.9	−8.44
20131025	11:00	17.6	7.69	378	8.1	−11.93	15.6	8.90	232	6.8	−11.93	18.6	8.35	338	6.2	−8.17
20131025	12:00	17.6	7.70	377	8.0	−11.77	17.1	9.18	234	3.0	−10.96	18.8	8.37	334	5.8	−8.22
20131025	13:00	17.5	7.70	377	8.0	−11.92	18.9	9.25	251	4.0	−10.26	20.1	8.37	332	6.8	−8.48
20131025	14:00	17.6	7.70	378	8.0	−13.04	20.7	9.27	221	4.5	−10.11					−9.12
20131025	15:00	17.5	7.70	378	8.0	−12.17	22.1	9.27	201	1.4	−9.92					−8.36
20131025	16:00	17.5	7.71	378	8.0	−12.64	25.0	10.29	190	17.0	−9.47					−8.73
20131025	17:00	17.5	7.71	377	8.1	−12.38	22.8	10.41	191	16.2	−10.07					−8.08
20131025	18:00	17.4	7.73	377	8.1	−12.06	21.8	9.83	180	12.6	−10.41					−8.11

$D^{14}C$ values were corrected for carbon isotopic fractionation using $\delta^{13}C$ values of the samples measured with ^{14}C by the AMS (Stuiver and Polach, 1977). The AMS ^{14}C counting statistical error for OXII is generally <0.5%, and all AMS ^{14}C dates are listed in Table 4.

3.6. Scanning electron microscopy (SEM)

Structures and elemental contents of some POC samples were analyzed by an Oxford Instruments Field Emission Scanning Electron Microscope (SEM) with an EMAX-ENERGY EDS system in the Department of Geosciences at National Taiwan University. The images and chemical compositions of some algae particles can be detected by the EDS-SEM. The results are shown in Fig. 12.

4. Results and discussion

4.1. Hydrochemistry of the spring-pond system

Table 1 shows the values of the measured water temperature, pH, EC, DO, Ca^{2+}, HCO_3^- and $\delta^{13}C_{DIC}$, as well as the calculated pCO_2 and SI_C values in January, July and October at each site. Data measured and samples collected from the different months represent hydrochemical conditions corresponding to soil activity and primary productivity in the study site under typical climatic conditions of different seasons, being January for winter, July for summer and October for autumn, respectively.

The measured results in Table 2 indicate that Ca^{2+} and HCO_3^- are the major cation and anion which come from dissolution of limestone and

Table 4
$\delta^{13}C$ and $D^{14}C$ values of the DIC, POC, and plant species from the karst water system. Aquatic plants, *Hydrilla verticillata, Charophyceae, Spirogyra* are submerged plants, whereas *Sparganium stoloniferum* is an emerged aquatic plant. For the DIC data, the sampling time is indicated in the bracket. See text for this discussion.

	Lab code	Type	$\delta^{13}C_{DIC}$ (‰)	$\delta^{13}C_{POC}$ (‰)	$\delta^{13}C_{plant}$ (‰)	pMC (%)	$D^{14}C$ (‰)	Age (yr BP)	Average
Spring									
January	NTUAMS-1991	DIC (12:00)	−11.18			93.12 ± 0.59	−68.8 ± 0.4	573 ± 51	
	NTUAMS-1049	POC				64.69 ± 0.86	−353.1 ± 4.7	3499 ± 107	
	NTUAMS-1553	*Hydrilla verticillata*			−22.68	96.99 ± 0.71	−30.1 ± 0.2	246 ± 59	
	NTUAMS-860	DIC (8:00)	−15.26			97.75 ± 0.78	−22.5 ± 0.2	183 ± 64	
July	NTUAMS-859	DIC (20:00)	−15.05			101.81 ± 0.63	18.1 ± 0.1	−144 ± 49	
	NTUAMS-1707	POC				54.66 ± 0.57	−453.4 ± 4.7	4853 ± 84	
	NTUAMS-1708	*Charophyceae*			−28.78	97.43 ± 0.76	−25.7 ± 0.2	209 ± 63	
	NTUAMS-857	DIC (8:00)	−12.36			97.12 ± 0.64	−28.8 ± 0.2	235 ± 53	
	NTUAMS-1191	POC		−28.80		79.19 ± 1.14	−208.1 ± 3.0	1875 ± 115	DIC
October	NTUAMS-1071	POC				71.56 ± 1.11	−284.4 ± 4.4	2688 ± 125	−25.5 ± 35.5
	NTUAMS-1491	*Charophyceae*			−34.53	86.75 ± 0.63	−132.5 ± 1.0	1142 ± 58	POC
	NTUAMS-1491-1	*Hydrilla verticillata*			−43.77	84.75 ± 1.01	−152.5 ± 1.8	1329 ± 95	−325 ± 104
Midstream pond									
	NTUAMS-1992	DIC (9:00)	−8.68			94.41 ± 0.65	−55.9 ± 0.4	462 ± 55	
	NTUAMS-858	DIC (12:00)	−11.77			109.51 ± 0.63	95.1 ± 0.6	−730 ± 46	
	NTUAMS-1583	DIC (18:00)	−6.75			104.02 ± 0.80	40.2 ± 0.3	−317 ± 62	
January	NTUAMS-1051-1	POC				82.50 ± 0.89	−175.0 ± 1.9	1546 ± 87	
	NTUAMS-1074	POC				72.94 ± 0.92	−270.6 ± 3.4	2535 ± 101	
	NTUAMS-1552	*Hydrilla verticillata*			−30.59	94.86 ± 0.79	−51.4 ± 0.4	424 ± 67	
	NTUAMS-1502	*Spirogyra*			−27.21	86.70 ± 0.80	−133.0 ± 1.2	1147 ± 74	
	NTUAMS-862-1*	DIC (8:00)	−15.15			93.34 ± 0.67	−66.6 ± 0.5	554 ± 58	
	NTUAMS-861	DIC (12:00)	−13.90			100.52 ± 0.58	5.2 ± 0.03	−42 ± 46	
July	NTUAMS-1069	POC				95.65 ± 0.76	−43.5 ± 0.3	357 ± 64	
	NTUAMS-1067	POC		−30.39		94.02 ± 1.06	−59.8 ± 0.7	495 ± 91	
	NTUAMS-1493	*Sparganium stoloniferum*			−28.52	105.25 ± 0.55	52.5 ± 0.3	−411 ± 42	
	NTUAMS-1060	DIC (12:00)	−10.96			99.73 ± 0.75	−2.7 ± 0.02	22 ± 60	
	NTUAMS-862	DIC (15:00)	−9.92			102.68 ± 0.51	26.8 ± 0.1	−213 ± 40	DIC
October	NTUAMS-1188	POC				87.61 ± 1.00	−123.9 ± 1.4	1063 ± 92	6.0 ± 55.9
	NTUAMS-1189	POC		−30.29		88.72 ± 1.01	−112.8 ± 1.3	962 ± 92	POC
	NTUAMS-1190	POC		−32.44		92.42 ± 0.98	−75.8 ± 0.8	633 ± 85	−123 ± 78.7
Downstream pond									
	NTUAMS-1914	DIC (18:00)	−7.93			103.01 ± 0.79	30.1 ± 0.2	−238 ± 62	
January	NTUAMS-1051	POC				66.19 ± 1.09	−338.1 ± 5.6	3315 ± 133	
	NTUAMS-1073	POC				82.73 ± 0.95	−172.7 ± 2.0	1523 ± 93	
	NTUAMS-1072	POC				74.39 ± 0.90	−256.1 ± 3.1	2377 ± 97	
	NTUAMS-844	DIC (8:00)	−12.38			91.02 ± 0.77	−89.8 ± 0.8	756 ± 68	
July	NTUAMS-1070	POC		−37.49		93.65 ± 0.90	−63.5 ± 0.6	527 ± 77	
	NTUAMS-1068	POC		−37.66		90.99 ± 1.04	−90.1 ± 1.0	758 ± 92	DIC
	NTUAMS-1915	DIC (8:00)	−8.93			105.65 ± 0.83	56.5 ± 0.4	−441 ± 63	0.3 ± 63.7
October	NTUAMS-1916	DIC (15:00)	−8.36			100.45 ± 0.81	4.5 ± 0.04	−36 ± 65	POC
	NTUAMS-1192	POC		−37.78		97.44 ± 1.07	−25.6 ± 0.3	208 ± 89	−158 ± 121

soil carbonate, so that the karst water system belongs to Ca-HCO_3^- type. These ions dominate the changes of the electrical conductivity (EC), shown by strong positive correlations between HCO_3^- and EC (Fig. 3a), and by generally positive trends for Ca^{2+} and EC (Fig. 3b). Previous studies have demonstrated that such positive correlations commonly exist in the karst water of the study area (Chen et al., 2014; Zhao et al., 2010, 2015a). Hence, variations of the measured EC can reflect changes in HCO_3^- concentration of the karst water. Fig. 3 shows that Ca^{2+} and HCO_3^- concentrations in the spring pool are generally higher than these in MP and DP, and the variation of Ca^{2+} and HCO_3^- concentrations in MP

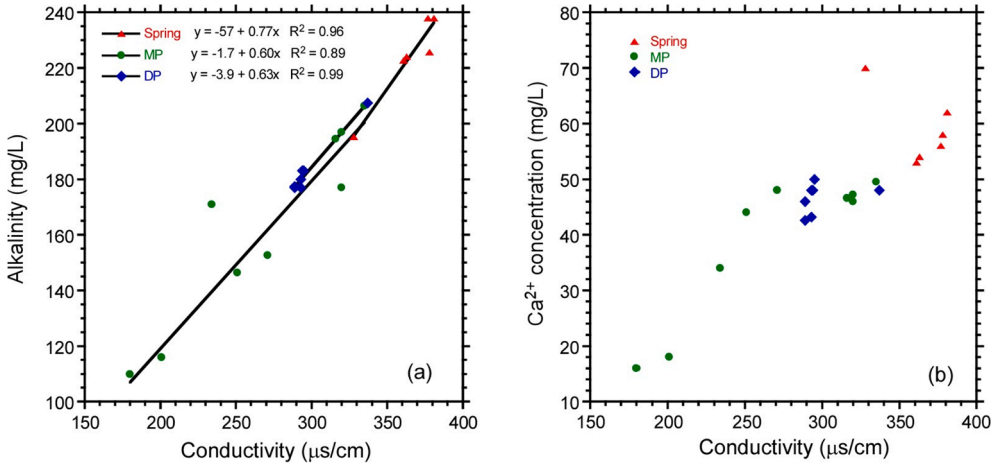

Fig. 3. (a) Correlations of EC and Alkalinity. (b) Relationship trends between EC and Ca^{2+}.

are much larger than these in DP. This is because the Ca^{2+} and HCO_3^- concentrations are affected by dilution, $CaCO_3$ precipitation (depending on buffering capacity of the carbonate system), atmospheric exchange, and biological productivity to a different extent for each site. In the study area, rainy season is in the summer. But, no rain event occurred during the sampling dates, so that dilution from surface runoff might be small. In fact, if dilution effect caused lower concentrations of Ca^{2+} and HCO_3^- in the spring-fed ponds, one would see lower Ca^{2+} and HCO_3^- concentrations in July, especially in the MP. However, this was not the case (Table 1). Since the input water of MP and DP came mainly from the spring, CO_2 degassing of the water will increase pH which might lead to $CaCO_3$ precipitation and decrease of Ca^{2+} and HCO_3^-. Biological uptake of CO_2 in MP and DP may further reduce the TCO_2 (i.e., total CO_2 including dissolve CO_2 gas, HCO_3^- and CO_3^{2-} ions). The consequence of those processes can be seen by changes in pH, SI_C and pCO_2 shown in Figs. 4 and 5. In Figs. 4a and 5d–f, the spring always has the lowest pH. Consequently, the calculated pCO_2 in the spring is higher than these in MP and DP, and SI_C is generally lower (Fig. 4b). The monitoring results also indicate that the spring water temperature (~2 °C variation) and EC (~10% variation) remained relatively constant through the year (Fig. 5), reflecting a relatively uniform source water. The summer spring water (7/24–25/2013) has the lowest pH and the highest pCO_2 with an unsaturated SI_C value (<0) (Table 1), probably because higher subsurface biological activity in soil during the summer added additional CO_2, as indicated by the more negative value for $\delta^{13}C$.

The above observations provide the following basic information: (1) The spring has relatively stable hydrochemical conditions over the course of the year, with stable water temperature, the lowest pH, highest EC (as well as Ca^{2+} and HCO_3^- concentrations) and high pCO_2; (2) Seasonally, there is a higher subsurface CO_2 contribution to the spring water during the summer causing lower pH, higher pCO_2 and unsaturated SI_C; (3) The absence of significant diurnal changes suggests very low biological activity and $CaCO_3$ precipitation occur in the spring pool; and (4) From the spring to MP and DP, loss of CO_2 from degassing, $CaCO_3$ precipitation and biological uptake change the hydrochemical conditions and isotopic composition of the DIC in the water. Based on these observations and carbon isotope values, we will discuss the carbon source and transformation processes.

Changes in the hydrochemical parameters and carbon isotopic compositions of MP and DP should have the similar trends and processes, considering that they have the same source water and environmental conditions. However, as mentioned above, the volume and depth of MP are much smaller than that of DP, so that the water residence time of MP is much shorter than that of DP. In MP, abundant submerged plants (dominated by ***Chara fragilis***) exist, whereas fewer aquatic plants exist in the spring and DP (Fig. 2). And, as shown by the diurnal changes, the primary productivity in MP is much stronger than that in DP (Fig. 5).

The diurnal hydrochemical variations of MP and DP (Fig. 5) will help in understanding controlling factors on the daily variations of DIC. During these monitoring days, there was no rainfall event to directly affect the hydrological condition. The pH is positively correlated with the water temperature. The EC varied negatively with T and pH. The variation patterns are similar in all seasons, so that one should not expect variation of seasonal soil CO_2 input to cause such changes. These daily changes should largely depend on CO_2 degassing, $CaCO_3$ precipitation, aquatic photosynthesis and respiration influenced by water temperature and sunlight (De Montety et al., 2011; Chen et al., 2014; Yang et al., 2015). As calculated earlier, the water residence time of SP, MP and DP were <1 h, 8–28 h and 7–25 days, respectively with much shorter time in July. One should consider the water replacement in MP. The water temperature increased from morning to late afternoon and then decreased continuously to the next morning. As water temperature increases, CO_2 degassing and $CaCO_3$ precipitation increase. Consequently, pH increases and EC (mainly HCO_3^- and Ca^{2+}) decreases. Aquatic photosynthesis increases during the daytime, while aquatic respiration occurs during the nighttime. The former process will take up CO_2, and the latter process will release CO_2. Compared to DP, the large variations of pH and EC in MP should be caused by much stronger aquatic photosynthesis and respiration in the smaller water body. The daily hydrochemical variation also provides insight to the changes in carbon isotopic composition.

4.2. $\delta^{13}C_{DIC}$ variation in the karst water system

Dissolved inorganic carbon (DIC) in the spring comes primarily from CO_2 released by organic matter oxidation and limestone bedrock dissolution in the subsurface. The DIC of the spring water is the main supply of the DIC in MP and DP. As water flows to MP and DP, CO_2 degassing, $CaCO_3$ precipitation, aquatic photosynthesis and respiration, and surface runoff dilution, can affect the DIC concentration and carbon isotopic fractionation. In a study of DIC behavior and $\delta^{13}C_{DIC}$ in three karst water catchments of Guizhou, Zhao et al. (2015a) summarized the factors influencing DIC concentration and $\delta^{13}C_{DIC}$, including (1) carbonate bedrock dissolution and $CaCO_3$ precipitation relative to water residence time, which is controlled by rates of groundwater flow, geomorphology, and initial pH of surface water; (2) soil CO_2 input controlled by vegetation, soil coverage and thickness, and land use; (3) exchange with atmospheric CO_2; and (4) aquatic plant photosynthesis and respiration in the water system.

$\delta^{13}C_{DIC}$ variations in the SP, MP and DP during each sampling period (Fig. 6) show several characteristics. First $\delta^{13}C_{DIC}$ values in the spring were lower than MP and DP during all sampling periods. Second, $\delta^{13}C_{DIC}$ values in all 3 settings were lower in July and October, and the highest in January. Third, $\delta^{13}C_{DIC}$ generally co-varies with pH in each reservoir,

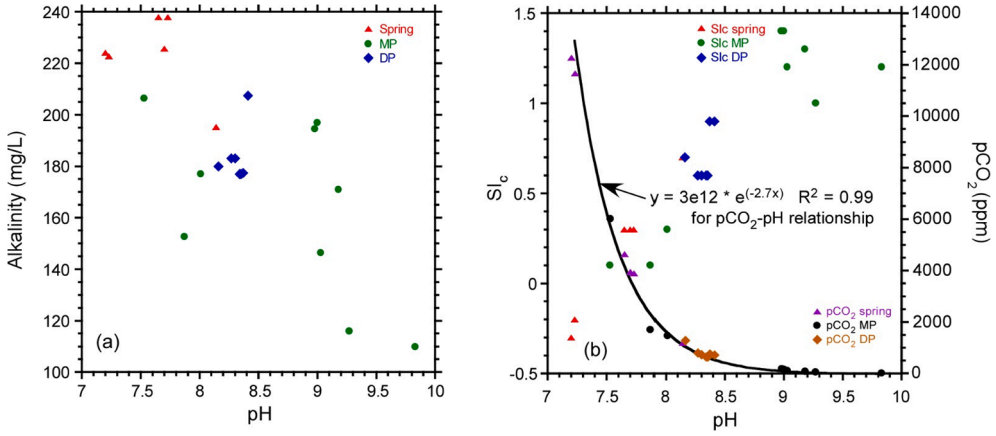

Fig. 4. (a) Relationship between Alkalinity and pH. (b) Relationships among pH, SI_C and pCO_2.

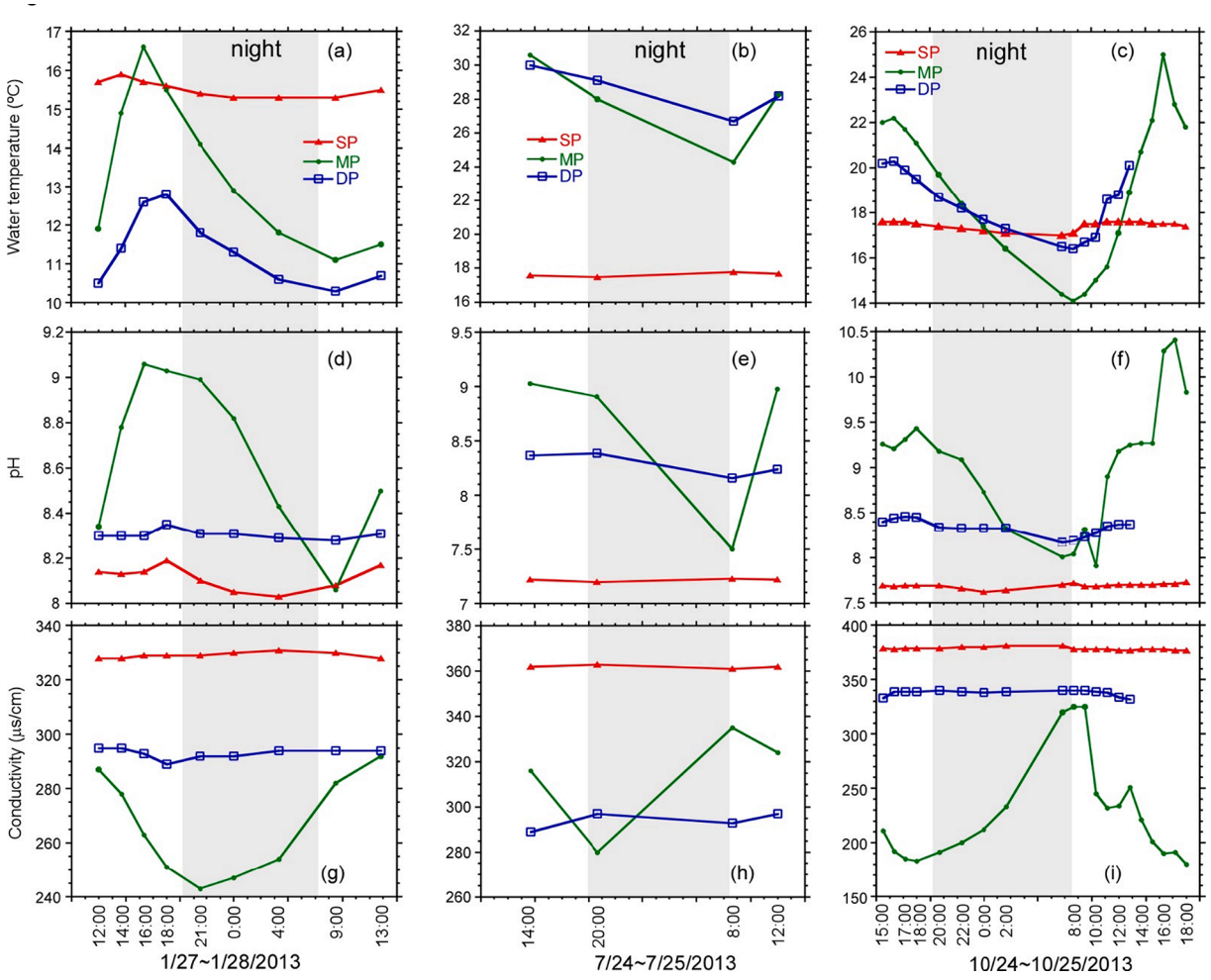

Fig. 5. Diurnal variations in water temperature, pH and EC in the spring, midstream and downstream ponds during three sampling periods. (a) January 27–28; (b) July 24–25; (c) October 24–25, 2013.

showing lower $\delta^{13}C_{DIC}$ corresponding to lower pH (Fig. 7). This finding agrees well with the results of Zhao et al. (2015a).

The above observations indicate that: (1) Assuming that decaying vegetation releases $\delta^{13}C_{DIC}$ with ~−25‰ and the limestone is near 0‰, DIC input to the spring comes mainly from soil CO_2 rather than limestone bedrock dissolution. (2) Groundwater input to MP and DP is negligible, and their DIC is mainly from the spring; (3) Dilution of TCO_2 by surface water runoff (rainfall) to the karst water system is minor. (4) The $\delta^{13}C$ of the source water is controlled by the soil CO_2 input, which is the major factor influencing seasonal $\delta^{13}C_{DIC}$ in each reservoir, with lower $\delta^{13}C$ in the summer rainy season. (5) The large diurnal variations of pH, EC, SI_C and pCO_2 in MP indicate that aquatic photosynthesis/respiration is much more important for the carbonate system than CO_2 degassing/$CaCO_3$ precipitation in MP. However, since the water residence time in MP is close to one day, part of the variations in MP is caused by inflow of spring water into the pond. The observation (4) can be demonstrated by the strong correlation of $\delta^{13}C_{DIC}$ - pH in the spring (Fig. 8a). The dominance of aquatic photosynthesis and respiration in MP reflects its abundant aquatic plant community. Considering HCO_3^- is the dominating ion in TCO_2, we use a plot of $\delta^{13}C_{DIC}$ - 1/[HCO_3] to illustrate the influence of aquatic photosynthesis. Fig. 8b shows that a strong correlation in MP indicates the effect of photosynthesis, although the relation may also be influenced by carbonate precipitation and CO_2 escape to the atmosphere.

The average $\delta^{13}C_{DIC}$ values with sample standard deviations for January 27–28, 2013 in the spring, MP and DP were −11.18 ± 0.11‰, −7.84 ± 0.94‰ and −7.95 ± 0.18‰, respectively (Table 3). In general, $\delta^{13}C$ of soil CO_2 in Guizhou ranges from −20‰ to −24‰ (unpublished data). The spring water TCO_2 should be a mixture of carbon released by soil respiration and dissolution of the carbonate bedrock. Assuming an average $\delta^{13}C$ of soil gas CO_2 in the study area is −22‰, the carbon isotopic fractionation at 20 °C will lead to 8.5‰ increase as it dissolves to become HCO_3^- (Chacko et al., 2001), so that the DIC in the surface water supplied from vadose zone respiration to the spring should have a $\delta^{13}C$ value around −13.5‰. Carbonate dissolution in the soil and through limestone bedrock along the passageway to the spring is a second source. Carbon isotopes in marine limestone and dolostone have been reported to range from −1‰ to 2‰ (Clark and Fritz, 1997), so $\delta^{13}C$ of the DIC from limestone dissolution should be around −1‰ (Chacko et al., 2001). The measured $\delta^{13}C_{DIC}$ of the spring is −11.18‰. Using the following simple mass balance equation, we can calculate the percentages of DIC from soil CO_2 (f_1) and limestone dissolution (f_2):

$$\delta_m \text{ (carbon isotope of the carbon mixture)} = f_{1\times}\delta_1 + f_{2\times}\delta_2 \quad (3)$$

$$f_1 + f_2 = 1 \quad (4)$$

where $\delta_m = \delta^{13}C_{DIC}$ ($\delta^{13}C$ of the DIC in the spring) = −11.18‰, δ_1 = −13.5‰, and δ_2 = −1‰. The carbon fraction from limestone dissolution is about 18.6%, whereas the carbon fraction from soil CO_2 is 81.4%. This mass balance calculation is quite different from the view implied by reaction (5) that would suggest DIC contribution in the karst water should come from an equal mixture of limestone dissolution and oxidized organic material (Hendy, 1971).

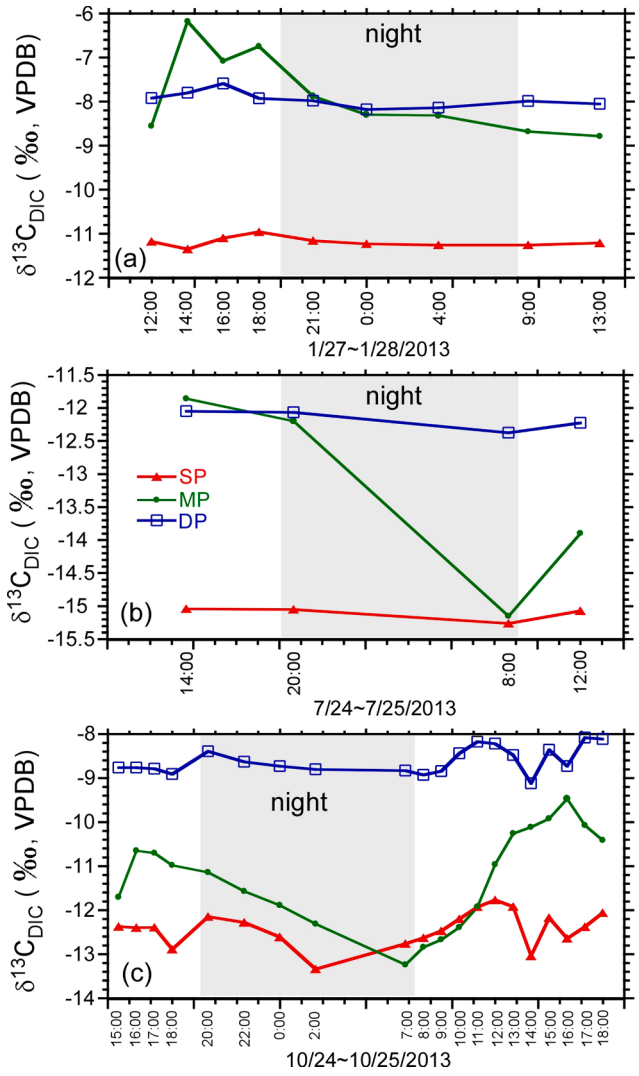

Fig. 6. Diurnal variations of $\delta^{13}C_{DIC}$ in Maolan spring and the two spring-fed ponds. (a) January 27–28; (b) July 24–25; (c) October 24–25, 2013.

$$H_2CO_3 + CaCO_3 \rightarrow Ca^{2+} + 2\,HCO_3^- \quad (5)$$

If this was the case, then the $\delta^{13}C$ of the spring water would be −7.25‰. In fact, many cave studies show that soil CO_2 is a major source of total CO_2 in cave and epi-karst waters and lighter $\delta^{13}C$ of cave and epi-karst waters in the summer is due to more contribution of soil CO_2 (e.g., Li et al., 2011, 2012; Zhao et al., 2015a). The $\delta^{13}C_{DIC}$ measurements of the spring pool indicates that the 18.6% contribution of carbonate dissolution is very likely under cooler water temperature and longer water residence time in the seepage path during the dry winter season.

High temperature in the rainy season leads to increased biomass productivity, strong root respiration and organic decomposition, providing more soil CO_2 with low $\delta^{13}C$ (Atkin et al., 2000). On the other hand, fast flow rate of seepage water reduces groundwater residence times, resulting in decreased carbonate dissolution per ml (Zhao et al., 2015a). The average $\delta^{13}C_{DIC}$ value of the spring in July 24–25 was −15.11 ± 0.11‰, with the lowest pH, negative SI_C and the highest pCO_2, confirming the above interpretations. Again, using −22‰ for the $\delta^{13}C$ of soil gas CO_2 and 30 °C for the summer temperature, the carbon isotopic fractionation between HCO_3^- (aq) and CO_2 (g) can be estimated (Chacko et al., 2001):

$$1000 ln\alpha_{HCO3-(aq)\ and\ CO2\ (g)} = -0.0945T(^{\circ}C) + 10.41 \quad (6)$$

An enrichment of 7.55‰ should exist from soil CO_2 to HCO_3^- in the seepage water. Thus, the estimated $\delta^{13}C$ of the seepage water should be about −15‰. As the measured $\delta^{13}C_{DIC}$ value of the spring is −15.11 ± 0.11‰, it means that carbon contribution of limestone bedrock dissolution in the summer is minor. If there is apparent CO_2 degassing and/or limestone bedrock dissolution in the seepage water, its $\delta^{13}C_{DIC}$ value should become heavier. $CaCO_3$ precipitation in the spring during July 24–25 was unlikely because $SI_C < 0$.

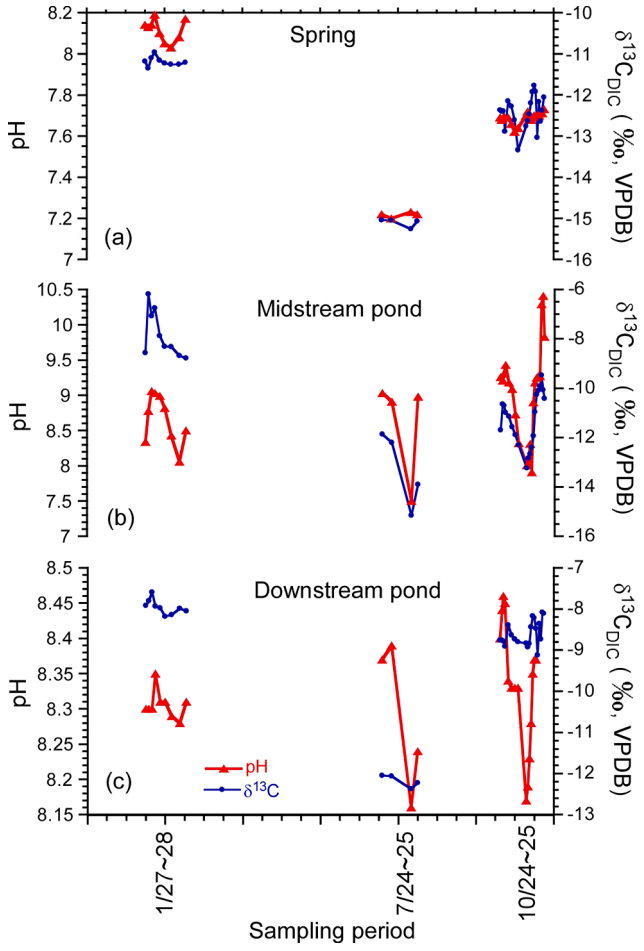

Fig. 7. Variations of $\delta^{13}C_{DIC}$ and pH in Maolan spring and the two spring-fed ponds through time. (a) Spring; (b) Midstream pond; (c) Downstream pond.

The average $\delta^{13}C_{DIC}$ value of the spring in October 24–25 was −12.42 ± 0.39‰ (n = 20). A similar estimation of the carbon contribution from soil CO_2 is >90%.

Comparing the $\delta^{13}C_{DIC}$ values between the spring and DP during the three sampling periods, about 3‰ enrichment in the $\delta^{13}C_{DIC}$ occurred from the spring to DP in each period, and the variation patterns of the $\delta^{13}C_{DIC}$ in the two reservoirs were very similar (Fig. 7). The 3‰ enrichment can only be explained by the following processes: (1) CO_2 degassing, (2) CO_2 exchange between DIC and the atmospheric CO_2, (3) increase CO_3^{2-}/HCO_3^- ratio due to pH increase, (4) aquatic photosynthesis, and (5) carbonate dissolution, since other processes such as $CaCO_3$ precipitation, aquatic respiration and organic decomposition lead to $\delta^{13}C_{DIC}$ depletion. Process (5) is unlikely because the SI_C values for DP are >0 (Table 1). Processes (1) to (3) occur simultaneously, but have different degrees of influences on carbon isotopic fractionation. CO_2 degassing leads to ^{12}C preferentially entering the atmosphere and pCO_2 decrease in the water, which results in pH increase and SI_C rise. The increased pH will further elevate the CO_3^{2-}/HCO_3^- ratio in the water that is Process (3) to have about 1‰ enrichment of $\delta^{13}C_{DIC}$ (Palmer et al., 2001). The pH increase and pCO_2 decrease from the spring to the spring-fed ponds support the Processes (1) and (3). Process (2), CO_2

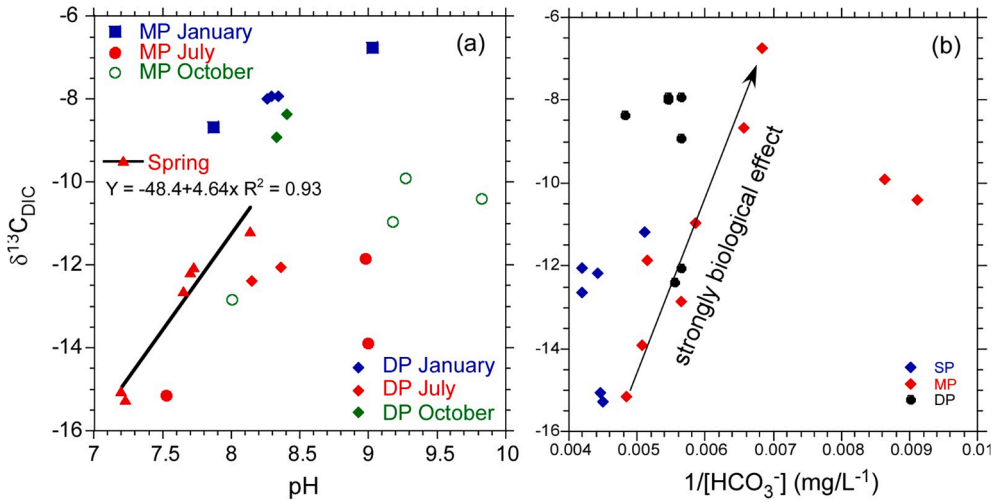

Fig. 8. Relationships of (a) $\delta^{13}C_{DIC}$ and pH, and (b) $\delta^{13}C_{DIC}$ and $1/[HCO_3^-]$. The left panel shows strong correlation of $\delta^{13}C_{DIC}$ and pH in the spring water, indicating the influence of CO_2 degassing/atmospheric exchange on the isotope change. The right panel exhibits strong correlation of $\delta^{13}C_{DIC}$ and $1/[HCO_3^-]$ in MP, reflecting the influence of biological activity on the isotope variation.

exchange between the DIC of the karst water and the atmospheric CO_2, is happening all the time. As the $\delta^{13}C$ of escaping CO_2 gas (about −22‰) in the spring is lighter than the $\delta^{13}C$ of atmospheric CO_2 (−8‰), Process (2) will lead to enrichment of $\delta^{13}C_{DIC}$ in the karst water. However, equilibrium CO_2 exchange would not affect pH of the karst water. Nevertheless, the influences of Processes (1) to (3) on the $\delta^{13}C_{DIC}$ change from the spring to the spring-fed ponds can happen simultaneously. Using $\delta^{13}C$ only, it is difficult to identify the relative importance of Processes (1) to (3).

Aquatic photosynthesis/respiration is an important process influencing isotopic composition. De Montety et al. (2011) pointed out that photosynthesis and respiration of aquatic plants are the dominant processes controlling in-stream diel isotopic variation. In daytime, a simultaneous increase of $\delta^{13}C_{DIC}$ and decrease of DIC indicates that photosynthesis is a primary control on DIC concentrations (Liu et al., 2015; Yang et al., 2015). Fig. 8 shows that correlation of $\delta^{13}C_{DIC}$ and pH in MP was not very strong (Fig. 8a), but correlation of $\delta^{13}C_{DIC}$ and $1/[HCO_3]$ in MP was rather strong (Fig. 8b), indicating the influence of biological activity on the isotopic signal in MP. In this karst water system, biological activity was relatively weak in the spring and DP, so that the influence of aquatic photosynthesis and respiration on their $\delta^{13}C_{DIC}$ was negligible, especially in winter time. However, diurnal variations of the $\delta^{13}C_{DIC}$ of the spring and DP during the October sampling period show some modest variation in both spring and DP reservoirs (Fig. 7c). Those variations in the $\delta^{13}C_{DIC}$ may not be attributed to aquatic photosynthesis and respiration in the water bodies. Instead, the variations may be caused by the $\delta^{13}C$ changes from the input water to the spring. Fig. 9 shows that the $\delta^{13}C_{DIC}$ of the spring and DP do not co-vary perfectly with their pH, EC and DO through time. Since the DIC of the spring comes mainly from the soil CO_2, its $\delta^{13}C_{DIC}$ variation may reflect $\delta^{13}C$ change in the soil water. For example, the decreased $\delta^{13}C_{DIC}$ during the night of October 24 might be attributed to low $\delta^{13}C$ of soil water due to plant respiration (shown by low DO and low pH) (Fig. 9).

In general, aquatic photosynthesis using CO_2 of DIC and producing oxygen will increase pH, CO_3^{2-}/HCO_3^- ratio and SI_C. This reduces pCO_2 and EC if $CaCO_3$ precipitates (Gattuso et al., 1999). The $\delta^{13}C_{DIC}$ of the water should increase as organic carbon formation preferentially uptakes ^{12}C (Yang et al., 1996). Aquatic plant respiration has the opposite effects. Therefore, if aquatic photosynthesis and respiration is significant, one should see above correlations among $\delta^{13}C_{DIC}$, pH, DO, SI_C, pCO_2 and EC. Fig. 10 demonstrates these correlations among $\delta^{13}C_{DIC}$, pH, DO, SI_C, pCO_2 and EC in MP where abundant aquatic plants exist.

During daytime, aquatic plants uptake CO_2 (aq) for photosynthesis,

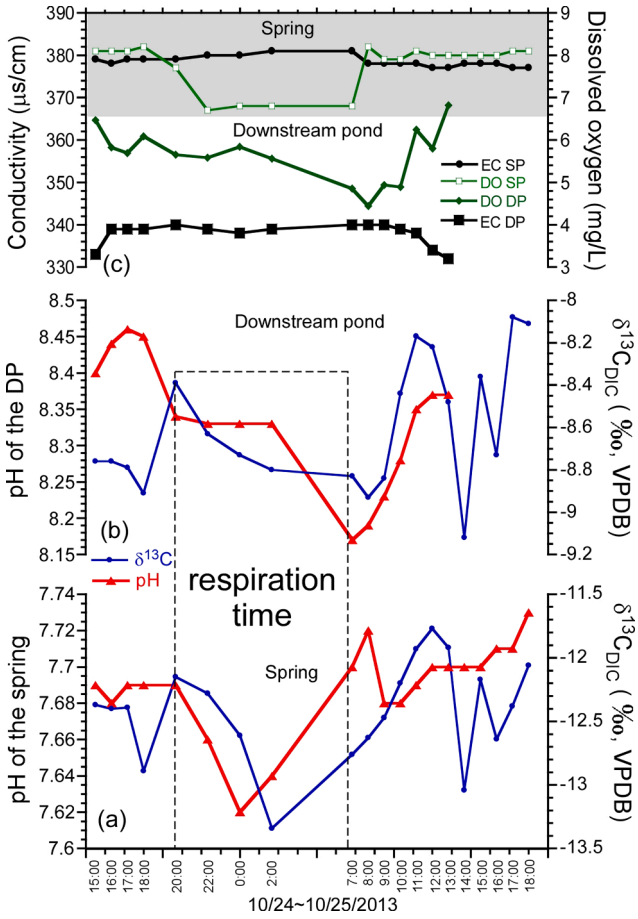

Fig. 9. Diurnal variations of $\delta^{13}C_{DIC}$, pH, EC and DO in Maolan spring and the downstream pond during October 24–25, 2013. (a) $\delta^{13}C_{DIC}$ and pH variations in the spring; (b) $\delta^{13}C_{DIC}$ and pH variations in the downstream pond; (c) EC and DO variations of the spring and DP.

facilitating precipitation of calcite; at night, on the other hand, respiration becomes the major process and produces CO_2 in the water that can cause the dissolution of calcite. Aquatic photosynthesis and respiration can be described by the following simplified reactions:

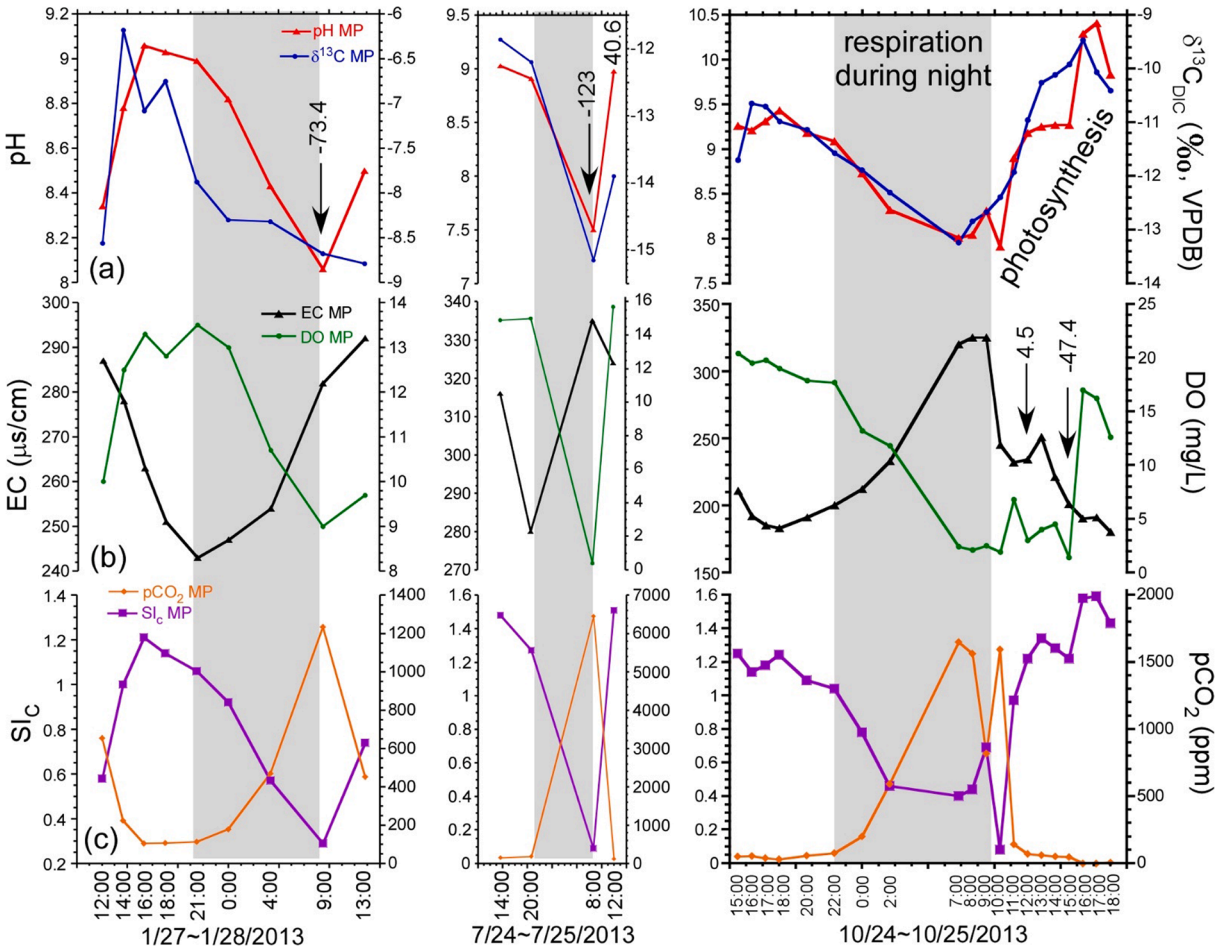

Fig. 10. Diurnal variations of $\delta^{13}C_{DIC}$ and hydrochemical parameters in the midstream pond during the three sampling periods. (a) pH and $\delta^{13}C_{DIC}$; (b) EC and DO; (c) SI_C and pCO_2. The numbers with arrows denote the $D^{14}C_{DIC}$ values.

$$Ca^{2+} + 2HCO_3^- \Rightarrow CaCO_3 + x\ (CO_2 + H_2O) + (1-x)\ (CH_2O + O_2)\ \text{(daytime)} \quad (7)$$

$$6H_2O + 6CO_2 \Rightarrow C_6H_{12}O_6 + 6O_2 \quad (8)$$

$$CaCO_3 + CO_2 + H_2O \Rightarrow Ca^{2+} + 2HCO_3^-\ \text{(night)} \quad (9)$$

$$C_6H_{12}O_6 + 6O_2 \Rightarrow 6H_2O + 6CO_2 \quad (10)$$

As discussed before, respiration in soil affects the $\delta^{13}C$, pH, EC and DO of the source water, bedrock dissolution, CO_2 degassing/exchange with the atmosphere, change of CO_3^{2-}/HCO_3^- ratio, $CaCO_3$ precipitation, aquatic photosynthesis/respiration, and all these can influence $\delta^{13}C_{DIC}$. However, these factors have different time scales and depend on biological conditions. Fig. 10 shows that change of soil respiration is the major factor controlling $\delta^{13}C_{DIC}$ and hydrochemistry on seasonal or longer time scales, with low $\delta^{13}C$, pH and DO, but high EC and pCO_2 in summer. In winter, both soil respiration and aquatic biological activity are less apparent. Changes in hydrochemical condition become dominant factors. The $\delta^{13}C_{DIC}$ of MP increased with increased water temperature, pH, CO_3^{2-}/HCO_3^- ratio and photosynthesis during daytime; the situation reversed during night time (Fig. 10). In addition, when biological activity is strong, the effect of CO_2 degassing becomes minor. For instance, CO_2 degassing should reach a maximum at noon on 10/25/2013, but the highest $\delta^{13}C_{DIC}$ appeared at 16:00, showing influence of photosynthesis on the $\delta^{13}C_{DIC}$.

4.3. $D^{14}C$ signatures of DIC in the karst water system

$D^{14}C$ expresses the $^{14}C/^{12}C$ ratio as (pMC – 1) × 1000, where pMC denotes fraction of modern carbon which is defined as the atmospheric ^{14}C in 1950 CE. In 1950 CE, pMC = 1 and $D^{14}C$ = 0‰. For a sample older than 60 ka, its pMC is close to zero and $D^{14}C$ = −1000‰. Owing to nuclear weapon testing in the atmosphere, its $D^{14}C$ reached to 800‰ in 1964, then started to decrease, primarily due to dilution as it mixed with other carbon reservoirs, including the terrestrial biosphere, the upper ocean and fossil fuel CO_2 input. In 2013, the atmospheric $D^{14}C$ was about 40‰ in North Hemisphere (Hua et al., 2013). Plants grown in land will have $D^{14}C$ values similar to that of the atmospheric CO_2. An emerged plant (*Sparganium stoloniferum* in Table 4) has $D^{14}C$ of 52.5 ± 0.3‰ which can represent the atmospheric $D^{14}C$ in the study site, although ^{14}C may be somewhat higher in the soil carbon pool that is decaying. If soil CO_2 is completely from decomposition of organic carbon (including plants and animals) which has the same $D^{14}C$ value as the atmospheric $D^{14}C$, its $D^{14}C$ is about 40‰. Considering DIC of the spring water comes from soil CO_2 and carbonate dissolution in the soil and along the seepage pass way, one may simply estimate the fractions of the two endmembers by the Eqs. (3) and (4). To make the model simple we do not consider the selective oxidation of young or old organic carbon, which could affect the ^{14}C mass balance.

The $D^{14}C_{DIC}$ values of the spring in January, July and October of 2013 were −68.8‰, −2.2‰ (average of −22.5‰ and 18.1‰) and −28.8‰, respectively (Table 4). Giving δ_1 = 40‰ (soil CO_2) and δ_2 = −1000‰ (limestone rock), then the contribution of soil CO_2 to the DIC in the spring in the January, July and October were 90%, 96% and 93%,

respectively. The percentage of limestone dissolution was <10%. If the $D^{14}C$ of the soil CO_2 is smaller than the atmospheric $D^{14}C$, then the estimated contribution of limestone dissolution should be even smaller. The mass balance calculation of the $D^{14}C$ supports the result of the $\delta^{13}C_{DIC}$. Nevertheless, estimation by the $D^{14}C_{DIC}$ shows the CO_2 contribution from carbonate dissolution to the DIC in the karst water system is <10%, and the contribution of soil CO_2 (or carbonate dissolution) is higher (or lower) in the summer time. The CO_2 of the DIC is mainly from soil CO_2. This result may provide constraints for radiocarbon dating of stalagmite samples (Li et al., 2015; Yin et al., 2017; Zhao et al., 2015b, 2017).

Compared to the spring, the $D^{14}C_{DIC}$ values of MP and DP should be higher (more positive) because CO_2 exchange with the atmosphere allows $D^{14}C_{DIC}$ to approach the atmospheric $D^{14}C$. The $D^{14}C_{DIC}$ values of MP and DP are complicated, as shown in Table 4 and Fig. 11. Sometimes the $D^{14}C_{DIC}$ values of the ponds were higher than these of the spring, but sometimes they were lower. As discussed before, CO_2 degassing, CO_2 exchange with the atmosphere, increased CO_3^{2-}/HCO_3^- ratio and photosynthesis will lead to increased $\delta^{13}C_{DIC}$, and $CaCO_3$ precipitation and respiration will cause $\delta^{13}C_{DIC}$ decrease. Among these processes, only CO_2 exchange with the atmosphere and respiration will influence $D^{14}C_{DIC}$. CO_2 exchange with the atmosphere always leads to increased $D^{14}C_{DIC}$. The influence of respiration on $D^{14}C_{DIC}$ depends on the CO_2 input from the respiration. If the CO_2 input from the respiration has a $D^{14}C$ value higher than the $D^{14}C_{DIC}$ of the water, the mixture will have higher $D^{14}C_{DIC}$. Otherwise, the mixture will have lower $D^{14}C_{DIC}$. Normally, respiration of terrestrial plants should provide a higher $D^{14}C$ value, but respiration of aquatic plants might not. It is interesting that the samples taken from both MP and DP in the mornings had lower $D^{14}C_{DIC}$ with lower $\delta^{13}C_{DIC}$, DO, and SIC values but high pCO_2, whereas the samples taken in the afternoons had higher $D^{14}C_{DIC}$ with relatively high $\delta^{13}C_{DIC}$, DO, and SI_C values but low pCO_2 (Table 3 and Fig. 10). The results clearly demonstrate the influence of CO_2 exchange with the atmosphere accompanied by CO_2 degassing and aquatic respiration. Since the aquatic respiration caused both $D^{14}C_{DIC}$ and $\delta^{13}C_{DIC}$ decreases especially in the summer time, one may expect that the $D^{14}C$ of the CO_2 decomposed from organic carbon is relatively low. However, whether the decomposed organic carbon which had low $D^{14}C$ comes from soil or in the aquatic system is unclear; the downstream pond should have weak aquatic respiration, but both $D^{14}C_{DIC}$ and $\delta^{13}C_{DIC}$ during the July sampling period show strong depletion, reflecting a significant amount of organic carbon decomposed. Therefore, it is possible that the CO_2 of respiration may come from older soil. Carbonate dissolution should not cause the $\delta^{13}C_{DIC}$ decrease, so it cannot be the mechanism to explain the decreased $D^{14}C_{DIC}$, especially in July and October.

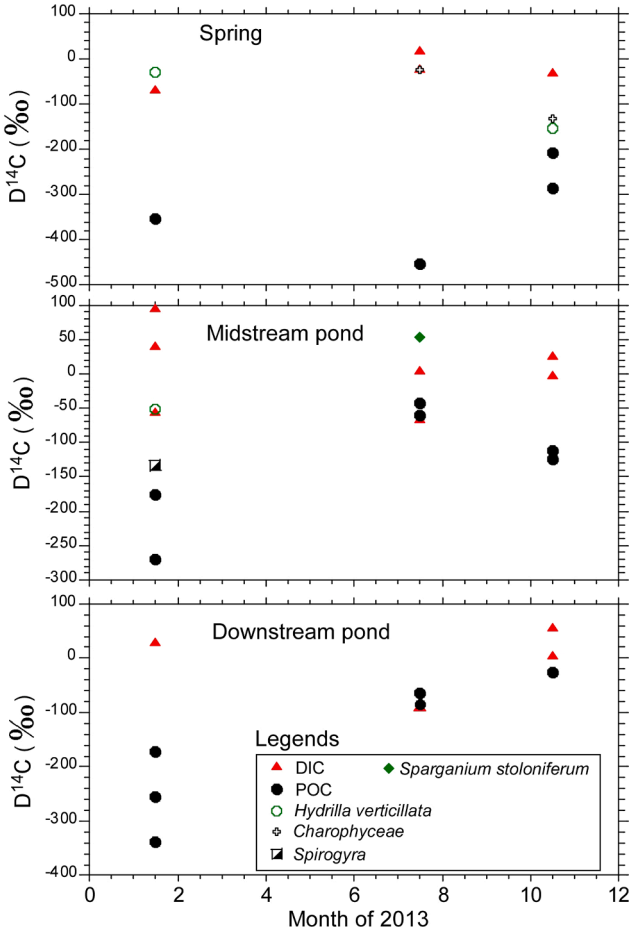

Fig. 11. $D^{14}C$ values of DIC, POC and aquatic plants in Maolan spring and the two spring-fed ponds.

4.4. $D^{14}C$ of POC in the karst water system

POC samples in this study were collected through 0.7 μm Whatman GF/F filter papers (47 mm in diameter) and consist of suspended particles in water. Sample weights are generally a few mg. The suspended particles include algae formed in the water, and detritus from aeolian dust and surface runoff. Since the algae are only a few μm in size, it is impossible to separate enough algae particles for AMS ^{14}C measurements. Therefore, the $D^{14}C_{POC}$ value is for the total organic carbon (TOC) of a POC sample.

The average $D^{14}C_{POC}$ values in the spring, MP and DP during January 27–28, 2013 were −353‰, −223‰ (average of −175‰ and −270.6‰) and −256‰ (average of three POC values), respectively, with a total average of −261 ± 77‰ ($n = 6$), much lower than $D^{14}C_{DIC}$ values for DIC in the corresponding sites (Table 4 and Fig. 11). It is not surprising that $D^{14}C_{POC}$ value of surface fresh water is lower than the atmospheric $D^{14}C$. For instance, Kao and Liu (1996) found that an average $D^{14}C$ value of POC samples from Lanyang Hsi (Lanyang River) was −875‰. The $D^{14}C_{POC}$ values of samples from Zhujiang and Xijiang rivers varied from −425‰ to −65‰ and −425‰ to −201‰, respectively (Wei et al., 2010; Sun et al., 2011; Liu et al., 2017). This is probably due to old organic carbon from detrital input through aerosol and surface runoff. Ishikawa et al. (2012) pointed out that the primary production in surface water transfers ^{14}C depleted carbon from carbonated rock into stream ecosystem food webs. Liu et al. (2017) also pointed out that POC is older than DIC in the Zhujiang River, consistent with a reservoir effect associated with POC "spiraling" (suspension/re-deposition) in streams and rivers. The absolute ages of DIC and POC in riverine systems are influenced by the geomorphic and hydrologic variations in different watersheds.

Besides POC "spiraling" (suspension/re-deposition) reason, CO_2 exchange with atmosphere is another reason for the $D^{14}C_{POC} <$ the $D^{14}C_{DIC}$ in the corresponding sites. DIC in the surface water can have strong CO_2 exchange with atmosphere, whereas POC cannot have CO_2 exchange with the atmosphere. Theoretically, if all POC were formed throughout photosynthesis by taking up dissolved CO_2 in the water (endogenous), their $D^{14}C$ values would be close to the $D^{14}C_{DIC}$ in the corresponding sites. However, all $D^{14}C_{POC}$ are much lower than the $D^{14}C_{DIC}$ in the corresponding sites, indicating the majority of POC comes exogenously from detritus. During the winter, primary productivity is low so that algae production can be also low. The EDS/SEM analyses shown in Fig. 12A provide such evidence, showing more detritus and low carbon contents in the January samples. Hence, the POC collected in January 27–28 of 2013 contains mainly detrital carbon which has older ^{14}C ages.

The $D^{14}C_{POC}$ values of the samples collected from MP and DP during July 24–25 and October 24–25 of 2013 range from −124‰ to −26‰ with an average of −74 ± 33‰ ($n = 8$). This average $D^{14}C_{POC}$ value is much higher than the average $D^{14}C_{POC}$ value of the winter samples (−223 ± 68‰), reflecting abundant algae formed in the ponds during

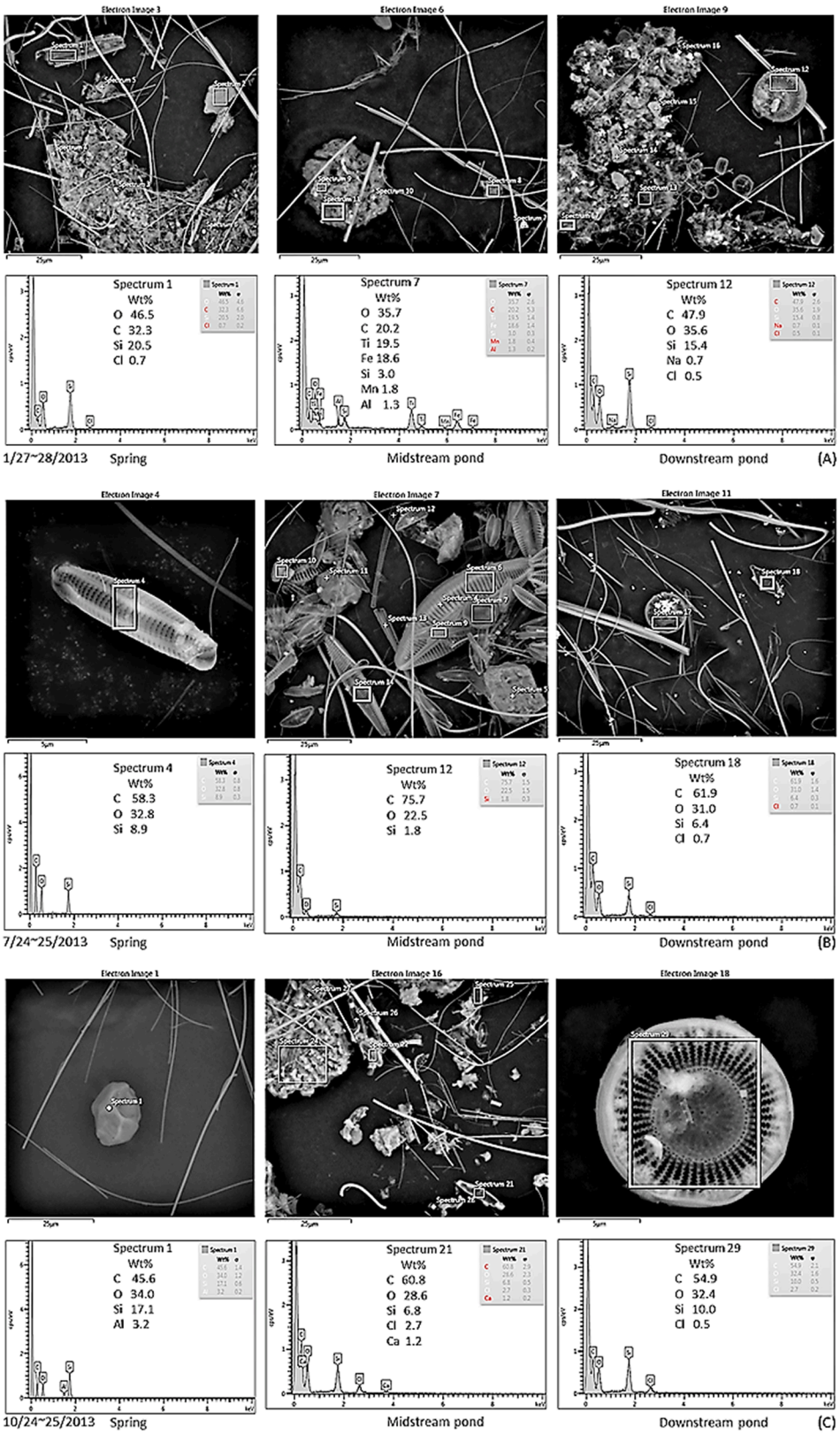

Fig. 12. EDS/SEM analysis of algae for the POC samples from the study site, (A): in January; (B): in July; (C): in October. The wire-like materials are glass fibers of the filter paper.

warm seasons. The EDS/SEM results show abundant algae and high C contents in the July from the ponds (Fig. 12B). As the $D^{14}C_{POC}$ of exogenous POC is unknown, however, currently we are not able to independently estimate how much POC was exogenous (surface runoff and aeolian dust). Because all the $D^{14}C_{POC}$ values are much lower than the atmospheric $D^{14}C$ even in MP during the summer time, our next question is whether the algae growing in the warm seasons uses DIC in the ponds or not. To answer this question, we need to know the $D^{14}C$ of

pure algae grown in the ponds. Unfortunately, we are unable to separate detrital POC and algae from a sample. And, even if the separation is possible, the amount of algae is not enough to date in the NTUAMS Lab. Nevertheless, the POC in the epi-karst system comes mainly from exogenous source in the winter time, but contains abundant algae (endogenous) in the spring-fed ponds during the warm seasons. The next section will show biological uptake of DIC through aquatic photosynthesis in the epi-karst system.

4.5. $D^{14}C$ signature of aquatic plants

The aquatic plants collected from the spring and MP are three submerged plants: *Hydrilla verticillata*, *Charophyceae* and *Spirogyra*, and one emerged plant: *Sparganium stoloniferum* (Table 4). The $D^{14}C$ values of the submerged plants range from -152.5 ± 1.8‰ to -25.7 ± 0.2‰ with an average of -87.5 ± 57.9‰ (n = 6), all significantly lower than the $D^{14}C$ value (52.5 ± 0.3‰) of the emerged plant which is equivalent to the local atmospheric $D^{14}C$. The results clearly demonstrate the submerged plants uptake their CO_2 from DIC in the water. If the submerged plants used atmospheric CO_2 only, then their $D^{14}C$ values should be close to that of emerged plants.

Nielsen (1946) determined that some plants could assimilate not only free CO_2 but also HCO_3^-. In fact, more and more studies demonstrate that aquatic plants uptake DIC for photosynthesis (e.g., Li et al., 2019; Blyakharchuk et al., 2020). Waterson and Canuel (2008) showed that the proportion from DIC transformation to TOC in the Mississippi River by aquatic photosynthesis could be 20% and 57% as revealed by lipid biomarker and $\delta^{13}C_{TOC}$ analyses. This loss of DIC will be partly transformed into organic carbon as stated in Eq. (7) (Sun et al., 2011), and eventually partly buried as autochthonous organic matter (Liu et al., 2011). This process constitutes a "biological carbon pump (BCP)" (De La Rocha and Passow, 2007; Liu et al., 2017) and increases the organic carbon preservation potential in the ponds (Liu et al., 2015). As Liu et al. (2015) suggested, if the terrestrial BCP effect is strong enough, as in the case of midstream pond (including both algae POC and plants), there is a carbon sink by drawing CO_2 directly from the atmosphere to surface water. This organic carbon is buried in the sediments, and its storage should be better quantified in the carbon cycle models.

Currently, quantitative estimation of the DIC fraction used for submerged plants during aquatic photosynthesis in the karst water system is limited by long-term measurements of $D^{14}C_{DIC}$ in a year. This study shows that the $D^{14}C_{DIC}$ varies during a day (Table 4), so that the $D^{14}C_{DIC}$ value used for photosynthesis of submerged plants is uncertain. We cannot use the $D^{14}C$ values of DIC and submerged plants in Table 4 for a mass balance calculation. However, one may ask why the $D^{14}C$ of the submerged plants in the spring pool during October (−132.5‰ and −152.5‰) was much lower than those during January (−30.1‰) and July (−25.7‰). In order to lower the $D^{14}C$ of the submerged plants, either the local atmospheric $D^{14}C$ or the $D^{14}C_{DIC}$ of the spring during autumn was lower. First of all, the study site is a forest environment far away from urban area, so there is no evidence that the local atmospheric $D^{14}C$ should be significantly lower. Second, if the submerged plants used only atmospheric CO_2 for photosynthesis, their $D^{14}C$ would be positive, and not related to $D^{14}C_{DIC}$ variation. Our hypothesis for the lower $D^{14}C$ of submerged plants in the spring during October is that the submerged plants have strong CO_2 uptake from DIC during photosynthesis and the long-term $D^{14}C_{DIC}$ in the spring was lower during late summer to autumn due to decomposition of organic matter shown by Reactions (9) and (10). Both POC (with $D^{14}C$ of −200‰~−450‰) decomposition and carbonate (with $D^{14}C$ of −1000‰) dissolution can contribute to low $D^{14}C$ CO_2. However, we think that the organic matter decomposition should be main reason as the $\delta^{13}C$ of the submerged plants were lower in October than those in January and July (Table 3).

Geyh et al. (1998) suggested that the primary ^{14}C sources in freshwater (aquatic) environments are atmospheric CO_2 exchange at the air-water interface and groundwater input of DIC. However, their explanation did not consider the process of carbon transformation. Our study indicates that (1) the majority of TCO_2 in the studied water comes from soil (biogenic) CO_2 rather than limestone dissolution; (2) submerged plants and algae formation through aquatic photosynthesis probably use larges amount of CO_2 from the DIC rather than the atmospheric CO_2 directly; and (3) aquatic photosynthesis in karst water can produce not only organic matter but also carbonate through the reactions shown by reactions (7) and (8). The carbon buried through this process is considered as a carbon sink. Nevertheless, our study illustrates that a strong biological pump effect in terrestrial surface waters should be considered as another important natural carbon sink, similar to the atmospheric CO_2 removal into the oceans (Ducklow et al., 2001; Passow and Carlson, 2012).

In addition, the ^{14}C ages of submerged plants are on the order of several hundreds and thousands of years. This means that plant remains from lake sediments and peat mires, especially in karst regions, may have initial ^{14}C ages. ^{14}C dating of aquatic plants should be done with caution.

5. Conclusions

Variations in hydrochemical data, $\delta^{13}C$ and $D^{14}C$ values of DIC, POC and plants in Maolan spring-pond system during January 27–28, July 24–25 and October 24–25 of 2013 have been studied. Influences of soil respiration adding CO_2, carbonate dissolution, CO_2 degassing and exchange with atmospheric CO_2, CO_3^{2-}/HCO_3^- ratio change, aquatic photosynthesis and respiration, and mixing of detrital carbon on temporal and spatial variations in $\delta^{13}C$ and $D^{14}C$ values of DIC, POC and plants have been discussed. Our understanding of the carbon source and processes in the karst water system can be summarized as follows:

1. CO_2 produced by respiration in soils is the major source for the DIC of the spring system, with higher input in the summer due to stronger biological activity under warm and wet conditions. Changes in soil CO_2 input is the major controlling factor for the variations of $\delta^{13}C$ and $D^{14}C$ on seasonal or longer scales. This discovery indicates that dissolution of CO_2 from the gas phase in soils is a significant factor in the carbon dynamic of this karst setting.
2. $\delta^{13}C$ and $D^{14}C$ have different behaviors during the processes of CO_2 degassing and exchange with atmospheric CO_2, CO_3^{2-}/HCO_3^- ratio change, carbonate dissolution and precipitation, and aquatic photosynthesis. $D^{14}C$ is a better carbon source indicator. When $\delta^{13}C$ and $D^{14}C$ are enriched simultaneously in the system, it reflects enhanced aquatic photosynthesis accompanied by CO_2 exchange with the atmospheric CO_2; whereas simultaneous depletion of $\delta^{13}C$ and $D^{14}C$ indicates plant respiration and/or organic matter decomposition. Diurnal variations of $\delta^{13}C_{DIC}$ in the karst water, aquatic photosynthesis and respiration have stronger influence than hydrochemical changes when the system has abundant aquatic plants. The mass balance estimate based on $D^{14}C_{DIC}$ results indicates that the contribution of respired soil CO_2 to the DIC in the spring may be >90%.
3. $D^{14}C_{POC}$ is much lower than the $D^{14}C_{DIC}$ value in the corresponding sites in the winter. This is due to effect of "spiraling" that introduces exogenous POC, but not attributed to DIC uptake. The increased $D^{14}C_{POC}$ values in warm seasons are attributed to greater algae formation which reduces the old carbon influence from the detritus.
4. Emerged aquatic plants use atmospheric CO_2 directly for organic carbon formation through photosynthesis, so that the initial ^{14}C age is small. However, submerged plants and algae primarily use DIC to form organic carbon through aquatic photosynthesis, so that they may have initial ^{14}C ages up to a few thousand years. The magnitude of carbon burial related to aquatic photosynthesis in fresh water systems should be re-evaluated in global carbon cycle budgets.

CRediT authorship contribution statement

Min Zhao, Bo Chen, Hao Yan, and Rui Yang conducted field work and lab work except AMS ^{14}C dating. Zhao and Li performed AMS ^{14}C dating, and generated the manuscript. Hong-Chun Li and Douglas E. Hammond finalized the manuscript and responded to the review comments.

Declaration of competing interest

The authors declare that they have no known competing financial interests or personal relationships that could have appeared to influence the work reported in this paper.

Acknowledgment

This work was supported by the funds from National Science Foundation of China (NSFC) (Grant No. 41673136, U1612441, 41807366), from the Strategic Priority Research Program of Chinese Academy of Sciences (Grant No. XDB40000000), from scientific platform talent project of Guizhou University of Finance and Economics (Grant No. [2018]5774-010) and from Ministry of Science and Technology of Taiwan (MOST) (Grant No. 104-2116-M-002-017 and 105-2116-M-002-010). We thank Dr. Zaihua Liu at Institute of Geochemistry, CAS, Guiyang for his funding support and initial project work.

References

Amiotte-Suchet, P., Aubert, D., Probst, J.L., Lafaye-Gauthier, F., Probst, A., Andreus, F., Viville, D., 1999. $\delta^{13}C$ pattern of dissolved inorganic carbon in a small granitic catchment: the Strenbach case study (Vosges mountains, France). Chem. Geol. 159, 129–145.

Atekwana, E.A., Krishnamurthy, R., 1998. Seasonal variations of dissolved inorganic carbon and $\delta^{13}C_{DIC}$ of surface waters: application of a modified gas evolution technique. J. Hydrol. 205, 265–278.

Atkin, O.K., Edwards, E.J., Loveys, B.R., 2000. Response of root respiration to changes in temperature and its relevance to global warming. New Phytol. 147, 141–154.

Aucour, A.M., Sheppard, S.M.F., Guyomar, O., Wattelet, J., 1999. Use of $\delta^{13}C$ to trace origin and cycling of inorganic carbon in the Rhône river system. Chem. Geol. 159, 87–105.

Blyakharchuk, T., Udachin, V., Li, H.-C., Kang, S.-C., 2020. Problem and high-resolution geochemical record in Manzherok Lake sediment core from Siberia: climatic and environmental reconstruction for Northwest Altai over the past 1,500 years. Front. Earth Sci. (Frontiers in Earth Sciences-Quaternary Science, Geomorphology and Paleoenvironment). 8, 206. https://doi.org/10.3389/feart.2020.00206.

Brock, F., Higham, T., Ditchfielf, P., Ramsey, C.B., 2010. Current pretreament methods for AMS radiocarbon dating at the oxford radiocarbon accelerator unit (ORAU). Radiocarbon. 52 (1), 103–112.

Buhl, D., Neuser, R., Richter, D., Riedel, D., Roberts, B., Strauss, H., Veizer, J., 1991. Nature and nurture: environmental isotope story of the river Rhine. Natur. wissenschaften. 78, 337–346.

Cassar, N., Laws, E.A., Bidigare, R.R., Popp, B.N., 2004. Bicarbonate uptake by Southern Ocean phytoplankton. Glob. Biogeochem. Cycles 18 (2), GB2003.

Chacko, T., Cole, D.R., Horita, J., 2001. Equilibrium oxygen, hydrology, and carbon isotope fractionation factors applicable to geologic systems. In: Valley, J.W., Cole, D. R. (Eds.), Stable Isotope Geochemistry, vol. 43. Mineralogical Society of America, Blacksburg, Virginia, pp. 1–81. Rev. Mineral. Geochem.

Chen, B., Yang, R., Liu, Z.H., Yan, H., Zhao, M., 2014. Effects of aquatic phototrophs on diurnal hydrochemical and $\delta^{13}C_{DIC}$ variations in an epikarst spring and two spring-fed ponds of Laqiao, Maolan, SW China. Geochimica. 43 (4), 375–385 (in Chinese with English abstract).

Clark, I.D., Fritz, P., 1997. Environmental Isotopes in Hydrogeology. *LEWIS*. Publishers, New York, pp. 111–136.

Das, A., Krishnaswami, S., Bhattacharya, S.K., 2005. Carbon isotope ratio of dissolved inorganic carbon (DIC) in rivers draining the Deccan Traps, India: sources of DIC and their magnitudes. Earth Planet. Sci. Lett. 2361, 419–429.

De Montety, V., Martin, J., Cohen, M., Foster, C., Kurz, M., 2011. Influence of diel biogeochemical cycles on carbonate equilibrium in a karst river [J]. Chem. Geol. 283, 31–43.

De La Rocha, C.L., Passow, U., 2007. Factors influencing the sinking of POC and the efficiency of the biological carbon pump. Deep Sea Res. Part II: Top. Stud. Oceanogr. 54, 639–658.

Degens, E.T., Kempe, S., Richey, J.E., 1991. Summary: biogeochemistry of the major world rivers. In: Degens, E.T., Kempe, S., Richey, J.E. (Eds.), Biogeochemistry of Major World Rivers, vol. 42. Wiley, New York, pp. 323–347. SCOPE Report.

Ducklow, H.W., Steinberg, D.K., Buesseler, K.O., 2001. Upper ocean carbon export and the biological pump. Oceanography. 14, 50–58.

Falkowski, P.G., 1997. Evolution of the nitrogen cycle and its influence on the biological sequestration of CO_2 in the ocean. Nature. 387, 272–275.

Falkowski, P.G., Raven, J.A., 2007. Aquatic Photosynthesis. Princeton University Press, Princeton.

Gattuso, J.P., Allemand, D., Frankigoulle, M., 1999. Photosynthesis and calcification at cellular, organismal and community levels in coral reefs: a review on interactions and control by carbonate chemistry. Amer. Zool. 39, 160–183.

Ge, T.T., Xue, Y.J., Jiang, X.Y., Zou, L., Wang, X.C., 2020. Sources and radiocarbon ages of organic carbon in different grain size fractions of Yellow River-transported particles and coastal sediments. Chem. Geol. 534 (1–11) https://doi.org/10.1016/j.chemgeo.2019.119452.

Geyh, M.A., Schotterer, U., Grosjean, M., 1998. Temporal changes of the ^{14}C reservoir effect in lakes. Radiocarbon. 42, 921–938.

Han, G.L., Tang, Y., Wu, Q.X., 2010. Hydrogeochemistry and dissolved inorganic carbon isotopic composition on karst groundwater in Maolan, southwest China. Environ. Earth Sci. 60, 893–899.

Hendy, C.H., 1971. The isotopic geochemistry of speleothems-I. The calculation of the effects of different modes of formation on the isotopic composition of speleothems and their applicability as paleoclimatic indicators. Geochim. Cosmochim. Acta 35, 801–824.

Hua, Q., Barbetti, M., Rakowski, A.Z., 2013. Atmospheric radiocarbon for the period 1950–2010. Radiocarbon 55 (4), 2059–2072.

Ishikawa, N.F., Uchida, M., Shibata, Y., Tayasu, I., 2012. Natural ^{14}C provides new data for stream food-web studies: a comparison with ^{13}C in multiple stream habitats. Mar. Freshw. Res. 63 (3), 21–217.

Ishikawa, N.F., Tayasu, I., Yamane, M., Yokoyama, Y., Sakai, S., 2015. Sources of dissolved inorganic carbon in two small streams with different bedrock geology: insights from carbon isotopes. Radiocarbon. 57 (3), 439–448.

Jiang, G., Guo, F., Wu, J., Li, H., Sun, H., 2008. The threshold value of epikarst runoff in forest karst mountain area. Environ. Geol. 55, 87–93.

Kanduč, T., Mori, N., Kocaman, D., Stibilj, V., Grassa, F., 2012. Hydrogeochemistry of Alpine springs from North Slovenia: insights from stable isotopes. Chem. Geol. 300, 40–54.

Kao, S.J., Liu, K.K., 1996. Particulate organic carbon export from a subtropical mountainous river (Lanyang Hsi) in Taiwan. Limnol. Oceanogr. 41 (8), 1749–1757.

Kuo, T.-S., Liu, Z.-Q., Li, H.-C., Wan, N.-J., Shen, C.-C., Ku, T.-L., 2011. Climate and environmental changes during the past millennium in central western Guizhou reflected by Stalagmite ZJD-21 record. J. Asian Earth Sci. 40, 1111–1120.

Li, H.-C., Tsai, C.-H., Zhao, M., Mii, H.-S., Chang, Q., Wei, K.-Y., 2015. The first high-resolution stalagmite record from Taiwan: climate and environmental changes during the past 1300 years. J. Asian Earth Sci. 114, 574–587.

Li, H.-C., Wang, J., Sun, J.-J., Chou, C.-Y., Li, H.-K., Xia, Y.-Y., Zhao, H.-Y., Yang, Q.-N., Sneha Kashyap, S., 2019. Study of Jinchuan Mire in NE China I: AMS ^{14}C, ^{210}Pb and ^{137}Cs dating on peat cores. Quater. Inter. 528, 9–17. https://doi.org/10.1016/j.quaint.2019.07.020.

Li, T.-Y., Shen, C.-C., Li, H.-C., Li, J.-Y., Chiang, H.-W., Song, S.-R., Yuan, D.-X., Lin, D.-J., Gao, P., Zhou, L.-P., Wang, J.-L., Ye, M.-Y., Tang, L.-L., Xie, S.-Y., 2011. Oxygen and carbon isotopic systematics of aragonite speleothems and water in Furong Cave, Chongqing, China. Geochim. Cosmochim. Acta 75, 4140–4156.

Li, T.-Y., Li, H.-C., Xiang, X.-J., Kuo, T.-S., Li, J.-Y., Zhou, F.L., Chen, H.L., Peng, L., 2012. Transportation characteristics of $\delta^{13}C$ in the plants-soil-bedrock-cave system in Chongqing karst area. Science China (D): Earth Sciences 55, 685–694.

Liu, H., Liu, Z.H., Macpherson, G.L., Yang, R., Chen, B., Sun, H.L., 2015. Diurnal hydrochemical variations in a karst spring and two ponds, Maolan Karst Experimental Site, China: biological pump effects. J. Hydro. 522, 204–417.

Liu, Z.H., 2013. Review on the role of terrestrial aquatic photosynthesis in the global carbon cycle. Procedia Earth and Planet. Sci. 7, 513–516.

Liu, Z.H., Dreybrodt, W., 2015. Significance of the carbon sink produced by H_2O-carbonate-CO_2-aquatic phototroph interaction on land. Sci. Bull. 60 https://doi.org/10.1007/s11434-014-0682-y.

Liu, Z.H., Li, Q., Sun, H.L., Wang, J.L., 2007. Seasonal, diurnal and storm-scale hydrochemical variations of typical epikarst springs in subtropical karst areas of SW China: soil CO_2 and dilution effects. J. Hydro. 337, 207–223.

Liu, Z.H., Dreybrodt, W., Wang, H.J., 2010. A new direction in effective accounting for the atmospheric CO_2budget: considering the combined action of carbonate dissolution, the global water cycle and photosynthetic uptake of DIC by aquatic organisms. Earth-Sci. Rev. 99, 162–172.

Liu, Z.H., Dreybrodt, W., Liu, H., 2011. Atmospheric CO_2 sink: silicate weathering or carbonate weathering? Appl. Geochem. 26, 292–294.

Liu, Z.H., Zhao, M., Min, Z., Sun, H.L., Yang, R., Chen, B., Yang, M.X., Zeng, Q.R., Zeng, H.T., 2017. "Old" carbon entering the South China Sea from the carbonate-rich Pearl River Basin: coupled action of carbonate weathering and aquatic photosynthesis. Appl. Geochem. 78, 96–104.

Marwick, T.R., Tamooh, F., Teodoru, C.R., Borges, A., Darchambeau, F., Bouillon, S., 2015. The Age of River-transported Carbon: A Global Perspective. AGU Publications, Global Biogeochemical Cycles, pp. 1–16. https://doi.org/10.1002/2014GB004911.

Meybeck, M., 1982. Carbon, nitrogen, and phosphorus transport by world rivers. Ameri. Sci. 282, 401–450.

Nielsen, E., 1946. Carbon sources in the photosynthesis of aquatic plants. Nature. 158, 594–596.

Palmer, S.M., Hope, D., Billett, M.F., Dawson, J.J.C., Bryant, C.L., 2001. Sources of organic and inorganic carbon in a headwater stream: evidence from carbon isotope studies. Biogeochem. 52, 321–338.

Passow, U., Carlson, C.A., 2012. The biological pump in a high CO_2 world. Mar. Ecol. Prog. Ser. 470, 249–271.

Raymond, P.A., Bauer, J.E., 2001a. DOC cycling in a temperate estuary: a mass balance approach using natural ^{14}C and $\delta^{13}C$ isotopes. Limnol. Oceanogr. 46 (3), 655–667.

Raymond, P.A., Bauer, J.E., 2001b. Use of ^{14}C and ^{13}C natural abundances for evaluating riverine, estuarine, and coastal DOC and POC sources and cycling: a review and synthesis. Org. Geochem. 32, 469–485.
Raymond, P.A., Bauer, J.E., 2001c. Riverine export of aged terrestrial organic matter to the North Atlantic Ocean. Nature. 409, 497–500.
Raymond, P.A., Bauer, J.E., Caraco, N.F., Cole, J.J., Longworth, B., Petsch, S.T., 2004. Controls on the variability of organic matter and dissolved inorganic carbon ages in northeast US rivers. Mar. Chem. 92, 353–366.
Stuiver, M., Polach, H.A., 1977. Discussion: reporting of ^{14}C data. Radiocarbon. 19, 355–363.
Sun, H.G., Han, J.T., Zhang, S.R., Lu, X.X., 2011. Transformation of dissolved inorganic carbon (DIC) into particulate organic carbon (POC) in the lower Xijiang River, S E China: an isotopic approach. Biogeosci. Discuss. 8, 9471–9501.
Sun, H.G., Han, J.T., Zhang, S.R., Lu, X.X., 2015. Carbon isotopic evidence for transformation of DIC to POC in the lower Xijiang River, SE China. Quater. Inter. 380-381, 288–296.
Taylor, C.B., Fox, V.J., 1996. An isotopic study of dissolved inorganic carbon in the catchment of the Waimakariri River and deep ground water of the North Canterbury Plains, New Zealand. J. Hydrol. 186, 161–190.
Tortell, P.D., Payne, C., Gueguen, C., Strezepek, R.F., Boyd, P.W., Rost, B., 2008. Inorganic carbon uptake by Southern Ocean phytoplankton. Limnol. Oceanogr. 53, 1266–1278.
Tsypin, M., Macpherson, G.L., 2012. The effect of precipitation events on inorganic carbon in soil and shallow groundwater, Konza Prairie LTER Site, NE Kansas, USA. Appl. Geochem. 27, 2356–2369.
Waterson, E.J., Canuel, E.A., 2008. Sources of sedimentary organic matter in the Mississippi River and adjacent Gulf of Mexico as revealed by lipid biomarker and $\delta^{13}C_{TOC}$ analyses. Org. Geochem. 39, 422–439.
Wei, X., Yi, W., Shen, C., Yechieli, Y., Li, N., Ding, P., Wang, N., Liu, K., 2010. ^{14}C as a tool for evaluating riverine POC sources and erosion of the Zhujiang (Pearl River) drainage basin, South China. Nucl. Inst. Methods Phys. Res. B 268, 1094–1097.
Wigley, T.M.L., 1977. WATSPEC: a computer program for determining equilibrium speciation of aqueous solutions. Br. Geomorphol. Res. Group Tech. Bull. 20, 1–46.
Xue, Y.J., Zou, L., Ge, T.T., Wang, X.C., 2017. Mobilization and export of millennial-aged organic carbon by the Yellow River. Limnol. Oceanogr. 62, S1), 95–111.
Yang, C., Telmer, K., Veizer, J., 1996. Chemical dynamics of the 'St. Lawrence' riverine system: $\delta^{18}D_{H2O}$, $\delta^{18}O_{H2O}$, $\delta^{13}C_{DIC}$, $\delta^{34}S_{sulfate}$, and dissolved $^{87}Sr/^{86}Sr$. Geochim. Cosmochim. Acta 60, 851–866.
Yang, R., Chen, B., Liu, H., Liu, Z.H., 2015. Carbon sequestration by terrestrial aquatic photosynthesis: insights from diurnal hydrochemical variations in an epikarst spring and two spring-fed ponds in different seasons. Appl. Geochem. 63, 248–260.
Yin, J.J., Li, H.-C., Rao, Z.G., Shen, C.-C., Mii, H.-C., Pillutla, R.K., Hu, X.M., Li, Y.X., Feng, X.H., 2017. Variations of monsoonal rain and vegetation during the past millennium in Tiangui Mountain, North China reflected by stalagmite $\delta^{18}O$ and $\delta^{13}C$ records from Zhenzhu Cave. Quater. Inter. 447, 89–101.
Zhao, M., Zeng, C., Liu, Z.H., Wang, S.J., 2010. Effect of different land use/land cover on karst hydrogeochemistry: a paired catchment study of Chenqi and Dengzhanhe, Puding, Guizhou, SW China. J. Hydrol. 388, 121–130.
Zhao, M., Liu, Z.H., Li, H.-C., Zeng, C., Yang, R., Chen, B., Yan, H., 2015a. Response of dissolved inorganic carbon (DIC) and $^{13}C_{DIC}$ to changes in climate and land cover in SW China karst catchments. Geochim. Cosmochim. Acta 165, 123–136.
Zhao, M., Li, H.-C., Mii, H.-S., Liu, Z.-H., Sun, H.-L., Shen, C.-C., 2015b. Changes in climate and vegetation of central Guizhou in southwest China since the last glacial reflected by stalagmite records from Yelang Cave. J. Asian Earth Sci. 114, 549–561.
Zhao, M., Li, H.-C., Shen, C.-C., Kang, S.-C., Chou, C.-Y., 2017. $\delta^{18}O$, $\delta^{13}C$, elemental content and depositional features of a stalagmite from Yelang Cave reflecting climate and vegetation changes since late Pleistocene in central Guizhou. China. *Quater. Inter.* 452, 102–115.
Zhou, Z., 1987. Scientific Survey of the Maolan Karst Forest. Guizhou Peoples' Publishing House, Guiyang, 385p. (In Chinese).